



Final Report SPR-FY22(003)

Asphalt Binder Laboratory Short-Term Aging - Phase II

Farzad Yazdipanah, M.S.

Graduate Research Assistant
Department of Civil and Environmental Engineering
University of Nebraska-Lincoln

Muhammad Ahmad, M.S.

Graduate Research Assistant

Zahra Kamali Khanghah, M.S.

Graduate Research Assistant

Mahdieh Khedmati, Ph.D.

Research Engineer

Jamilla Teixeira, Ph.D.

Assistant Professor

Mohammad Ghashami, Ph.D.

Assistant Professor (Adjunct)

Hamzeh F. Haghshenas, Ph.D.

Research Assistant Professor

Nebraska Department of Transportation Research

Headquarters Address (402) 479-4697
1400 Nebraska Parkway <https://dot.nebraska.gov/business-center/research/>
Lincoln, NE 68509
ndot.research@nebraska.gov

Nebraska Transportation Center

262 Prem S. Paul Research (402) 472-1932
Center at Whittier School <http://ntc.unl.edu>
2200 Vine Street
Lincoln, NE 68583-0851

This report was funded in part through grant from the U.S. Department of Transportation Federal Highway Administration. The views and opinions of the authors expressed herein do not necessarily state or reflect those of the U.S. Department of Transportation.

Asphalt Binder Laboratory Short-Term Aging – Phase II

Farzad Yazdipanah, M.S.
Graduate Research Assistant
Department of Civil & Environmental
Engineering
University of Nebraska-Lincoln

Muhammad Ahmad, M.S.
Graduate Research Assistant
Department of Civil & Environmental
Engineering
University of Nebraska-Lincoln

Zahra Kamali Khanghah, M.S.
Graduate Research Assistant
Department of Mechanical and Materials
Engineering
University of Nebraska-Lincoln

Mahdieh Khedmati, Ph.D.
Research Engineer
Department of Civil & Environmental
Engineering
University of Nebraska-Lincoln

Jamilla Emi Sudo Lutf Teixeira, Ph.D.
Assistant Professor
Department of Civil & Environmental
Engineering
University of Nebraska-Lincoln

Mohammad Ghashami, Ph.D.
Assistant Professor (Adjunct)
Department of Mechanical and Materials
Engineering
University of Nebraska-Lincoln

Hamzeh F. Haghshenas, Ph.D.
Research Assistant Professor
Department of Civil & Environmental
Engineering
University of Nebraska-Lincoln

Sponsored By

Nebraska Department of Transportation and US Department of Transportation Federal Highway
Administration

December 2024

Technical Report Documentation Page

1. Report No. SPR-FY22(003)		2. Government Accession No.		3. Recipient's Catalog No.	
4. Title and Subtitle Asphalt Binder Laboratory Short-Term Aging – Phase II				5. Report Date October 15, 2024	
				6. Performing Organization Code	
7. Author(s) Farzad Yazdipناه, Muhammad Ahmad, Zahra Kamali Khanghah, Mahdieh Khedmati, Jamilla Teixeira, Mohammad Ghashami, Hamzeh Haghshenas				8. Performing Organization Report No. If applicable, enter any/all unique numbers assigned to the performing organization.	
9. Performing Organization Name and Address University of Nebraska-Lincoln Department of Civil Engineering 362M Whittier Research Center Lincoln, NE 68583-0856				10. Work Unit No.	
				11. Contract	
12. Sponsoring Agency Name and Address Nebraska Department of Transportation 400 Highway 2 PO Box 94759 Lincoln, NE 68509				13. Type of Report and Period Covered Final Report 07/2022 - 10/2024	
				14. Sponsoring Agency Code	
15. Supplementary Notes					
16. Abstract <p>This study examined the effectiveness of laboratory short-term aging processes for warm mix asphalt (WMA) binders using response surface methodology (RSM) with various combinations of aging parameters: time, temperature, airflow, and binder weight. The research aimed to enhance understanding of aging parameter efficacy and propose a modified laboratory short-term aging protocol that accurately simulates plant short-term aging in WMA binders. Additionally, the study explored the potential of thermal simulation techniques to model the heat transfer within asphalt mixtures during the compaction procedure. To achieve these goals, three WMA mixtures produced at 135 °C were collected from plants, and their asphalt binders were extracted and recovered. Virgin binders from the same projects were also obtained and two of them aged in a rolling thin film oven at different combinations of aging parameters, designed by RSM. High-temperature performance grade and carbonyl index were used as model responses to quantify laboratory aging levels. These parameters were also assessed in the plant extracted binders to establish target values. The statistical analysis revealed significant effects of time, temperature, and weight, as well as their interactions, on key rheological and chemical properties of binders, while the airflow rate effect within the studied range was found to be insignificant. Two distinct modified protocols for laboratory short-term aging of WMA binders produced at 135 and 165 °C were developed, showing consistency with plant short-term aged binder results. The models were successfully validated using chemical and rheological assessments of a third binder aged with the proposed protocols. Thermal simulation results indicated that the average allowable time window for compaction increased slightly with the use of finer aggregates and thicker asphalt binder films around the aggregates. Using the available critical window of time for effective compaction ensures the compaction procedure is conducted within the optimal temperature range, leading to more durable pavement layers.</p>					
17. Key Words Short-term Aging; Rolling Thin Film Oven; Warm Mix Asphalt; Response Surface Methodology; Rheological Properties, Chemical Characterization, Thermal Modeling			18. Distribution Statement No restrictions. This document is available through the National Technical Information Service. 5285 Port Royal Road Springfield, VA 22161		
19. Security Classification (of this report) Unclassified		20. Security Classification (of this page) Unclassified		21. No. of Pages 55	22. Price

Form DOT F 1700.7 (8-72)

Reproduction of completed page authorized

Abstract

This study examined the effectiveness of laboratory short-term aging processes for warm mix asphalt (WMA) binders using response surface methodology (RSM) with various combinations of aging parameters: time, temperature, airflow, and binder weight. The research aimed to enhance understanding of aging parameter efficacy and propose a modified laboratory short-term aging protocol that accurately simulates plant short-term aging in WMA binders. Additionally, the study explored the potential of thermal simulation techniques to model the heat transfer within asphalt mixtures during the compaction procedure. To achieve these goals, three WMA mixtures produced at 135 °C were collected from plants, and their asphalt binders were extracted and recovered. Virgin binders from the same projects were also obtained and two of them aged in a rolling thin film oven at different combinations of aging parameters, designed by RSM. High-temperature performance grade and carbonyl index were used as model responses to quantify laboratory aging levels. These parameters were also assessed in the plant extracted binders to establish target values. The statistical analysis revealed significant effects of time, temperature, and weight, as well as their interactions, on key rheological and chemical properties of binders, while the airflow rate effect within the studied range was found to be insignificant. Two distinct modified protocols for laboratory short-term aging of WMA binders produced at 135 and 165 °C were developed, showing consistency with plant short-term aged binder results. The models were successfully validated using chemical and rheological assessments of a third binder aged with the proposed protocols. Thermal simulation results indicated that the average allowable time window for compaction increased slightly with the use of finer aggregates and thicker asphalt binder films around the aggregates. Using the available critical window of time for effective compaction ensures the compaction procedure is conducted within the optimal temperature range, leading to more durable pavement layers.

Disclaimer

The contents of this report reflect the views of the authors, who are responsible for the facts and the accuracy of the information presented herein. The contents do not necessarily reflect the official views or policies neither of the Nebraska Department of Transportations nor the University of Nebraska-Lincoln. This report does not constitute a standard, specification, or regulation. Trade or manufacturers' names, which may appear in this report, are cited only because they are considered essential to the objectives of the report.

The United States (U.S.) government and the State of Nebraska do not endorse products or manufacturers. This material is based upon work supported by the Federal Highway Administration under SPR-FY22(003). Any opinions, findings and conclusions or recommendations expressed in this publication are those of the author(s) and do not necessarily reflect the views of the Federal Highway Administration.

This report has been reviewed by the Nebraska Transportation Center for grammar and context, formatting, and 508 compliance.

Acknowledgments

The authors would like to thank the Nebraska Department of Transportation (NDOT) for the financial support needed to complete this study. In particular, the authors thank NDOT Technical Advisory Committee (TAC) for their technical support and invaluable discussions/comments. The authors would also like to thank Mr. Nitish Bastola for his efforts on sample collection in this project.

Table of Contents

Technical Report Documentation Page	ii
Abstract	iii
Disclaimer	iv
Acknowledgments	v
Table of Contents	vi
List of Figures	vii
List of Tables	viii
Chapter 1 Introduction and Background	1
1.1 Objectives	8
1.2 Methodology	9
1.3 Organization of the Report	12
Chapter 2 Materials and Methods	13
2.1 Materials	13
2.1.1 Sample Collection	13
2.1.2 Asphalt Binder and Warm Mix Asphalt (WMA) additives	17
2.2 Methods	17
2.2.1 Asphalt Binder Extraction Method	17
2.2.2 Standard Short-Term Aging (STA)	18
2.2.3 High-Temperature Performance Grade (PG)	19
2.2.4 Carbonyl Index Determination	20
2.2.5 Elemental Analysis	21
2.3 Experimental Design Using Response Surface Methodology (RSM)	21
Chapter 3 Results and Discussion	24
3.1 Asphalt Binder Characterization Based on Standard RTFO Protocol	24
3.2 Effects of RTFO Parameters on Binder Properties	25
3.3 Model Fitting	26
3.4 Proposed Modified RTFO Protocol	31
3.5 Validation of the Modified RTFO Protocols	35
Chapter 4 Thermal Simulation	37
Chapter 5 Conclusions and Recommendation	47
References	49

List of Figures

Figure 1.1 Experimental plan in this study	10
Figure 2.1 Site locations associated with different projects	13
Figure 2.2 Sample collection process at the site plant.	14
Figure 2.3 Asphalt binder extraction process stages.....	18
Figure 2.4 The DSR test setup for the High-temperature continuous PG measurement	19
Figure 2.5 The FTIR test setup and equipment in this study	21
Figure 3.1 Properties of unaged, plant aged (135 and 165 °C), and laboratory aged binders (a) high-temperature PG and (b) IC=O	25
Figure 3.2 Interaction plots of RTFO parameters for B2: (a) IC=O and (b) high-temperature PG	30
Figure 3.3 Contour plots: (a) high-temperature PG of B1, (b) high-temperature PG of B2, (c) IC=O of B1, and (d) IC=O of B2.....	32
Figure 3.4 High-end PG and IC=O of B3 aged in the field, and with the current and proposed STA protocols: (a) first scenario and (b) second scenario	36
Figure 4.1 Schematic representation of heat dissipation from a 63 mm (pre-compression) asphalt mixture with an initial temperature of 176 °C.	38
Figure 4.2 Illustration of the normal distribution of aggregate sizes within the asphalt mixture.	42
Figure 4.3 The time in which the mixture needs to reach $T = 135^{\circ}\text{C}$ after the application the roadway for (a) 75 μm aggregate with an average time of $\approx 11':45''$ and $\approx 13':05''$ for 4 μm and 13 μm binder, respectively, (b) 19.5 mm aggregate diameter with an average time of $\approx 9':52''$ and $\approx 10':40''$ for 4 μm and 13 μm binder, respectively, and (c) randomized aggregate sizes with an average time of $\approx 10':41''$ and $\approx 11':40''$ for 4 μm and 13 μm binder, respectively.	43
Figure 4.4 Temperature-depth profiles of asphalt layers. Each graph represents the temperature distribution at the specified time when the average temperature of the mixture reaches 135°C . The solid line marks the vertical position of 135°C , while the temperature at various depths demonstrates the cooling rate of each layer based on aggregate size (a) smallest aggregate, (b) largest aggregate, (c) distributed aggregate sizes.	45

List of Tables

Table 1.1 Reduction in gaseous emissions of WMA projects as compared to HMAs [15].	2
Table 2.1 Properties of the studied asphalt binders, WMA additives, and plant produced mixtures	16
Table 3.1 Input parameter arrangement and response values for laboratory-aged asphalt binders	26
Table 3.2 ANOVA table for B1 and B2 binders: High-end PG and IC=O	27
Table 3.3 Combination of parameters as alternative RTFO protocol for WMA binders produced at 135 °C (first scenario)	33
Table 4.1 Thermal and physical properties of inclusion materials in asphalt mixture	40

Chapter 1 Introduction and Background

Highway infrastructure covers over eight million lane miles in the United States. The predominant surface materials are asphalt and Portland cement concrete mixtures [1], with asphalt mixtures constituting more than 90% of US paved roads [2]. With respect to production temperature, two primary types of asphalt mixtures applicable for paving purposes are hot mix asphalt (HMA) and warm mix asphalt (WMA) mixtures [3, 4]. These asphalt mixtures differ in their production methods, processing temperatures, compositions, formulations, and in-service performance [5]. HMA production involves a process with required mixing and compaction temperatures ranging from 150° C to 190 °C. The process starts with heating the asphalt binder and aggregates in a fueled furnace until achieving the specified temperature. The heating process continues until the asphalt mixture is delivered to paving sites on loaded trucks. Consequently, the high manufacturing temperatures and resulting fumes create a toxic and hazardous environment for the workforce and laborers [1]. Thus, the HMA production steps are considered non-environmentally friendly, costly, and time-consuming [6]. Furthermore, upon the completion of paving and compaction processes, the pavements cannot be used immediately until achieving a completely dry surface. It should also be noted that in many climate regions, the paving process of HMA is only feasible during warmer seasons. Therefore, the overall process of HMA production is expensive, time consuming, and potentially detrimental to human health [7].

The implementation of WMA technology was initially introduced in Europe following the Kyoto treaty on climate change, with the objective of reducing greenhouse gas emissions [8]. Low viscosity binders with higher workability and pumpability, derived in a shorter time frame, made the asphalt pavement manufacturing process possible at lower temperatures [9, 10]. Generally, WMA operates within the temperature range of 115-135 °C, making it a viable

substitution to HMA without compromising pavement performance [11]. The most significant advantages associated with WMA technology include conservation of fossil fuels, reduction of greenhouse gas emissions and energy consumption, provision of improved working condition at plant sites, reduction of binder aging, and extension of construction season [12, 13]. A study conducted by Gandhi et al. in 2008 documented the gaseous emissions from WMA projects, demonstrating significantly lower emissions compared to those of the HMAs [14]. Table 1.1 indicates two important WMA technologies and their corresponding reductions in emissions as compared to HMA.

Table 1.1 Reduction in gaseous emissions of WMA projects as compared to HMAs [15].

Sr. No	Emission	Evotherm	Sasobit
1.	Carbon Dioxide	81%	-
2.	Sulfur Dioxide	46%	18%
3.	Carbon Monoxide	-	63%
4.	Nitrogen Oxide	54%	34%

Regardless of the method employed in asphalt pavement production, the aging of asphalt mixtures is an inevitable phenomenon that begins during production and continues throughout its service life. Asphalt mixture aging is a complex process wherein the mechanical and chemical properties of asphalt binder change over time, affecting the performance of the asphalt mixture [16]. The main mechanisms involved in binder aging are volatilization, oxidation, and steric hardening [17]. Volatilization and oxidation result from alterations in the molecular structure, while steric hardening is a consequence of molecular rearrangement [18]. The temperature increment during production, storage, transport, and placement of asphalt mixture triggers

volatilization. When the asphalt temperature exceeds 150 °C, it initiates the volatilization of specific bitumen fractions, and each additional heating increment of 10-12 °C has the potential to double the rate of volatilization [19]. This volatilization phenomenon can potentially increase the binder viscosity, with some studies reporting increases of up to 200% [20]. Oxidation results from the interaction of complex organic compounds within the bitumen and is further influenced by atmospheric oxygen and UV radiation. This oxidation process contributes to increased brittleness and the emergence of cracks within the asphalt layer [21]. Steric hardening of bitumen gradually occurs at room temperature, leading to a molecular rearrangement within the bitumen [22]. This physical hardening results in augmented viscosity and the manifestation of volume contractions.

The aging process typically initiates at the earliest stages of asphalt mixture production when the asphalt binder and aggregates are mixed in the fuel-fired rotating mixers, transported, and laid into the pavement mat, and continues throughout the service life of the pavement [23]. The aging that occurs during the asphalt construction period, including the mixing, transportation, paving, and compaction of asphalt mixture, is designated as short-term aging (STA); whereas the aging that happens after the pavement operation stage and during its service life is termed long-term aging (LTA) [24, 25, 26, 27].

The laboratory evaluation of asphalt aging not only simulates the STA and LTA of asphalt binder but also serves as a preliminary step for numerous chemical and mechanical characterizations of the asphalt binder, i.e., performance grading via bending beam rheometer (BBR) and dynamic shear rheometer (DSR) tests. For STA simulation, two laboratory tests, thin film oven test (TFOT), and rolling thin film oven (RTFO) test are considered the most reliable methods. In 1940, TFOT was introduced to differentiate asphalts in terms of volatility and

characteristics. This test simulates the STA by heating a film of asphalt binder in an oven for five hours at a temperature of 163 °C (ASTM D1754). The RTFO was developed by the California division of highways and adopted by ASTM in 1970 to age the asphalt binder in thinner films than the 1/8 inches used in TFOT [28]. The RTFO procedure, developed during the Strategic Highway Research Program (SHRP), was employed to predict short-term oxidative aging during the production and implementation of HMA. Following ASTM D2872, a bottle in a rotating carriage is filled with 35 g of binder and subjected to an airflow of 4000 ml/min for 85 minutes at a temperature of 163 °C. Similar to field conditions during HMA production, a thin film of asphalt binder is continuously exposed to heat and air during the RTFO procedure. As a result, the level of oxidative aging was reported to be adequately comparable to what occurs in actual HMA production, and the changes in chemical and mechanical properties observed in the field can be predicted using the RTFO protocol [29].

While the complex conditions of an actual asphalt plant cannot be precisely replicated, extensive experience demonstrated that the level of oxidative hardening induced by the RTFO is adequately representative of that occurring for HMA at modern continuous-feed drum mixer facilities [30]. However, the standard RTFO procedure was originally developed for unmodified asphalt binders utilized in HMA production [31, 32]. Research in recent years has shown some deficiencies related to the RTFO test. Firstly, the residual amount of asphalt recovered from the RTFO test is minimal, and the glass bottle is difficult to clean, which reduces the efficiency of the test. Secondly, due to the differences in viscosity, mixing temperatures, storage time, and paving time, the RTFO's short-term aging protocol is unsuitable for the highly viscous binder such as polymer modified asphalt, warm mix asphalt, and additive based asphalt binders [33, 34, 35, 36]. The problems are mainly due to improper dispersion of binder inside the bottles and

creeping of highly viscous binder out of the bottle during rotation [37]. To improve the RTFO test method, several studies have been conducted to date. Bahia et al. [38] proposed using a steel rod placed in the glass bottle to generate additional shear forces to resolve the improper dispersion of highly modified binders during the RTFO aging procedure. Consequently, the film was forced to diffuse more evenly, and the bottle was expected to be easier to clean. However, an investigation on this modified RTFO performed by FHWA indicated that the metal rods reduced RTFO aging of modified asphalts and caused the asphalt binder to drop out of the glass bottles [39]. A study conducted by Haghshenas et al. stated that the binders modified by the polymers or other varieties of additives, age differently compared to traditional HMA [40]. The different behavior is identifiable through rutting, aging index, and viscosity tests of laboratory and field aged asphalt binders [41, 42, 43, 44].

With the implementation of performance-based designs and the increase in innovation in asphalt mix design production, WMA technology has gained acceptance across the United States, with 45 states actively using WMA additives in their major paving mix designs and trial projects [30, 45, 46]. Several studies have reported that WMA experiences different levels of STA compared to HMA [47, 48, 49, 50, 51, 52]. More specifically, recent studies have raised doubts about standard RTFO capabilities in simulating asphalt binder STA during WMA production in the field [53, 54]. That said, the sufficiency of this method for simulating STA of modified binders produced using different technologies such as WMA technology is questionable [55]. The higher viscosity of modified binders, improper dispersion throughout the bottles, creeping of binders out of rotating bottles, and various levels of binder aging experienced at different production temperatures might be primary reasons for potential discrepancies [56], [57].

Zhang et al. stated that the standard RTFO aging method is not sufficient to simulate field short-term aging conditions in binder modified with WMA additives such as Sasobit and Evotherm [27]. Ferrotti et al. investigated water foamed WMA binders in terms of chemical and rheological characteristics after short-term aging. Based on the results, it was suggested to find an appropriate aging temperature for the RTFO procedure in the case of WMA foamed binders [58]. A study conducted by Arafat et al. reported that RTFO aging cannot be directly correlated with plant aging for WMA binders and some adjustments on RTFO protocol are necessary depending on the actual field condition [41]. In another study with WMA additives applied in rubberized binders, the standard RTFO temperature reduced by 18°C (same as the reduction in WMA production temperatures), with the chemical and morphological results showing more compatibility of this method with the unaged binders [59]. Wasiuddin et al. evaluated the effects of time and temperature on the RTFO procedure to simulate the lower aging level in WMA binders. However, in lieu of field results, short-term oven aging of laboratory-produced mixtures were utilized to develop an STA model [31]. Overall, it is evident that WMA binders and mixtures are not adequately and correctly characterized in terms of laboratory short-term aging. This is important because the simulation of field short-term aging in the laboratory is a preliminary step for many rheological characterizations of the asphalt binder, such as performance grading by the bending beam rheometer (BBR) and dynamic shear rheometer (DSR) tests. Further, Nebraska is one of the eminent states using WMA technology in their asphalt mixture design. With that, the appropriate laboratory STA simulation of WMA binders is a priority for the state.

A survey on previous literature indicates that the effects of time and temperature have been the center of attention in the study of short-term oxidative aging [2, 3]. Various parameters

are involved in oxidative short-term aging, with the most significant being time, temperature, binder weight, and airflow [32, 60, 61]. However, careful selection of short-term aging parameter values is crucial for accurately simulating the short-term aging process of WMA mixtures, particularly when these parameters can be influenced by interactions with other factors. On the other hand, it is reported that RTFO can adequately simulate short-term aging; however, the current RTFO protocol is inefficient in the simulation of highly viscous binders (polymer modified binders and Performance Grade (PG) 70-XX and higher grade binders) due to improper dispersion throughout the bottles and creeping of highly viscous binder out of the bottles during rotation [4, 5]. In addition, there are some doubts about the capability of RTFO in the simulation of the oxidative aging process that occurs during warm mix asphalt (WMA) production [6, 7]. Also, the capability of the RTFO protocol to accurately mimic short-term aging of asphalt binders treated by recycling agents (RAs) is questionable.

The PI and Co-PI proposed a research project entitled “Asphalt Binder Laboratory Short-Term Aging” to statistically investigate the effect of time, temperature, airflow rate, and asphalt binder weight on the chemical and rheological properties of different asphalt binders in the laboratory short-term aging (RTFO) process. In addition, it was attempted to find an improved RTFO aging protocol, which was applicable on both unmodified and highly modified binders. The statistical analysis showed that the first order terms of time, temperature, and weight as well as their interactive terms were statistically significant. However, the effect of airflow rate, within the studied range, was insignificant. Based on the findings of the first part of the study, a new/improved protocol was proposed in which the aging duration was reduced to 45 min while the temperature increased to 180°C. In addition, only 25 g of binder and an airflow rate between 3 and 5 L/min were required for conducting the new short-term laboratory-aging process.

According to the obtained rheological properties as well as the chemical characteristics, it was shown that the proposed laboratory short-term aging protocol can not only reduce the aging time of the conventional protocol but is also applicable to both neat and polymer-modified modern asphalt binders.

In continuation with the previous research project, finding short-term aging parameters (i.e., new/improved protocol) that can properly simulate the aging process during WMA production is vital since nearly all the asphalt mixtures in our state are produced using WMA technology. Also, there is a need for better understanding the short-term aging of asphalt binders treated by RAs since NDOT is planning to use these chemical additives in Nebraska asphalt mixtures in the near future.

Using strategies for the design of experiment (DOE), such as response surface methodology (RSM) implemented with central composite design (CDD), and statistical techniques to analyze the results, the individual and interaction effects of different parameters can be acquired [62], [63], [64]. Analyzing different parameters and their interactions with respect to real field aging may result in different levels of RTFO parameters for WMA binders, effectively proposing a new or alternative aging protocol.

1.1 Objectives

Considering the anticipated use of WMA and modified asphalt binders, the current complications with the WMA short-term aging protocol, and the discrepancies between the actual and simulated STA by the RTFO test for WMA binders, this study aims to propose the optimization of RTFO's short-term aging process for potential application with WMA binders. The main objectives of this study can be listed as:

- Understanding the effect of RTFO parameters, i.e., time, temperature, airflow, and weight

of binder, on rheological and chemical properties of binder with WMA additives.

- Proposing a new/improved RTFO aging protocol applicable on binders with WMA additives considering their production temperatures.

1.2 Methodology

To achieve the objectives, different chemical and rheological characterization of binders were considered in an experimental plan (Figure 1.1), along with statistical analysis techniques.

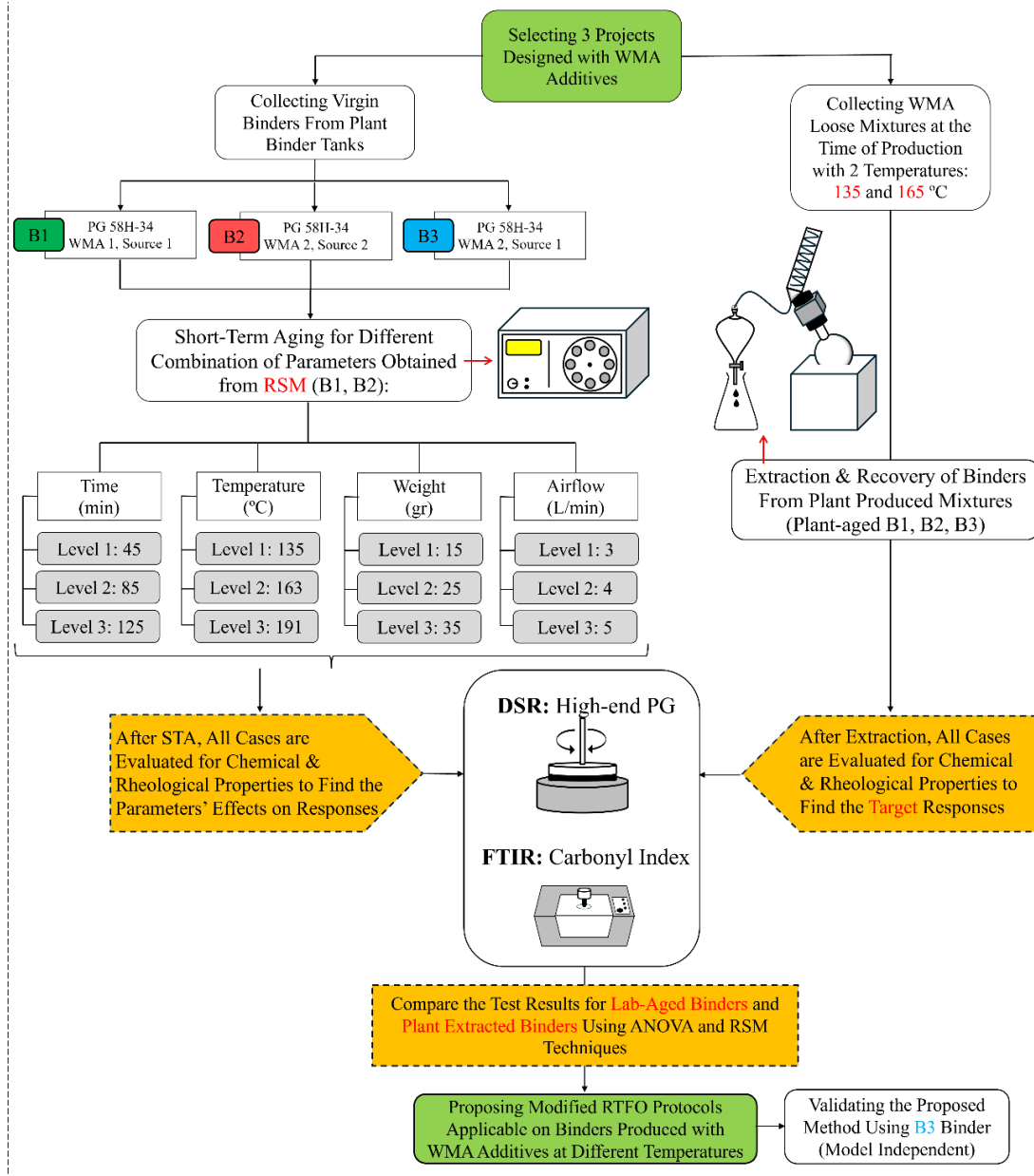


Figure 1.1 Experimental plan in this study

As the first step, three plant-produced asphalt mixtures designed with WMA binders were collected to be the field short-term aged loose mixtures (at two temperatures of 135 and 165 °C). After the binder extraction and recovery, the dynamic shear rheometer (DSR) and Fourier

Transform Infrared Spectroscopy (FTIR) tests were conducted on the recovered binders to determine the target high-temperature PG and carbonyl index (IC=O), respectively.

In the second step, the virgin binders used in the same asphalt mixtures and collected from the tank at the time of mixture production underwent thorough attempt at laboratory short-term aging to investigate the effect of time, temperature, airflow, and binder weight (inside the bottles) on the short-term aging and RTFO results. The RSM approach followed by statistical analysis was used to design the experiment and find an alternative laboratory short-term aging protocol that can accurately simulate the STA of WMA binders with respect to the field data. Generally, WMA mixtures are produced at lower temperatures, however, in Nebraska they are produced at a similar temperature to HMA and used as a compaction aid. For this reason, the field sample collection was conducted at two different temperatures (135 and 165 °C), and the RTFO optimization was performed for two scenarios: Producing WMA at 135 °C, and producing WMA at 165 °C.

In the third step, the new/improved protocol was validated using a third binder to determine its applicability for different types of WMA binders. To accomplish this, the third binder aged by the new/improved RTFO method was evaluated in terms of high-temperature PG and IC=O and the results were compared to the target values derived from the same field aged binder. This chemo-physical approach was conducted to show whether the proposed method results in a similar aging process as the real field short-term aging.

Furthermore, this study seeks to investigate the temperature profile within an asphalt layer during the compaction process. To achieve this objective, various heat transfer scenarios considering different specifications and thermal properties of materials are evaluated to determine the temperature profile and rate of heat transfer in an asphalt layer. The potential

promising results from this modelling can predict and optimize the available time window for the compaction procedure (explained in detail in Chapter 4). The overall process of RTFO optimization and asphalt layer temperature profile prediction is anticipated to save time, cost, energy, and material, as well as lead to a higher quality field pavement layer. It might also provide the state DOT with improved quality control and quality assurance measures for future asphaltic pavements. For a better understanding of the report and adopted procedures, Figure 1.1 illustrates the schematics of the experimental plan for STA optimization of WMA binders in this study.

1.3 Organization of the Report

This report includes five chapters. In Chapter 1, the introduction and background are presented along with the objects and methodology employed herein. Chapter 2 presents the selected materials and experimental methods used in this study. Chapter 3 presents the experimental outcomes and discussion on the findings, as well as presenting results for the validation of the modified RTFO method proposed. Chapter 4 presents thermal simulations considering different scenarios, specifications, results and discussion. Finally, Chapter 5 summarizes the main conclusions from this research, possible implementation plans, and recommendations for future studies.

Chapter 2 Materials and Methods

2.1 Materials

2.1.1 Sample Collection

Three Surface Laminate X-Treme Thin (SLX) asphalt mixtures produced with WMA additives and used in the state of Nebraska were selected in this study. Plant produced mixtures and tank binder were collected from different Nebraska project locations. Figure 2.1 shows the site locations associated with different projects.



Figure 2.1 Site locations associated with different projects

The first type of asphalt mixture and binder collected was for the project N-121, Crofton North, NE, USA utilizing PG 58H-34 and 0.7% Evotherm® as the WMA additive. The loose mixtures were collected prior to the addition of any RAP to the drum, and the asphalt mixture and associated binder were named M-B1 and B1, respectively. The second mixture type was employed at the US-30 and US-81 intersection, Columbus East & North, NE, USA. This SLX

asphalt mixture type was produced with PG58H-34 (obtained from Flint Hills) and 0.7% Delta S® and was collected before the addition of any RAP to the mixture. The same binder used for the mixture production was also collected from the binder tank during this process. This asphalt mixture and associated binder were named M-B2 and B2, respectively. Figure 2.2 presents the sample collection process at the site plant.



Figure 2.2 Sample collection process at the site plant.

The third site for sample collection was on US-77 in Pickrell North, NE, USA using the SLX type of asphalt mixtures. The asphalt binder employed was PG58H-34 (obtained from Flint Hills), modified with 0.7% Evotherm® as the WMA additive, and no RAP was utilized in mixture production at the time of sample collection. This asphalt mixture and associated binder were named M-B3 and B3, respectively.

The sample collection was divided into two stages: loose mixture collection from site plants and binder collection from binder tanks. For the former, the production temperature in the plant was controlled to meet the production temperature conditions for WMA and HMA mixtures. Accordingly, samples were collected at two production temperatures: 135 °C and 165 °C, for subsequent binder extraction purposes, and these samples were designated M-B1, M-B2, and M-B3. For the latter stage, the same asphalt binders were collected from the binder tanks for the laboratory short-term aging conditioning, and these samples were named B1, B2, and B3. In total, three different types of asphalt mixtures produced at two different temperatures were evaluated in this study. Two of these asphalt mixtures (B1 and B2) were used for the development of the modified protocols, and the third one (B3) was employed to validate the proposed method. Table 2.1 provides information across asphalt mixtures and binders (extracted or collected from tanks) used in this study.

Table 2.1 Properties of the studied asphalt binders, WMA additives, and plant produced mixtures

Asphalt Binder			
Binder ID	B1	B2	B3
Supplier	Source 1 (Jebro)	Source 2 (Flint Hills)	Source 2 (Flint Hills)
Contractor	Knife River Midwest	Western Engineering	Werner Construction
Project Location	N-121, Crofton North	US-30 & US-81, Columbus East & North	US-77, Pickrell North
Continuous High-Temperature PG (°C)	61.3	63.8	64.8
PG (°C)	PG 58H-34	PG 58H-34	PG 58H-34
<i>Elemental Analysis (%)</i>			
Carbon	82.46	84.08	82.54
Hydrogen	10.52	10.14	10.03
Nitrogen	0.59	0.66	0.61
Oxygen	1.67	0.73	1.65
Sulfur	3.28	8.15	4.38
WMA Additives			
WMA type	Evotherm	Delta-S	Evotherm
Density (gr/cm ³)	0.98	0.93	0.98
Flash Point (°C)	200	298	200
Viscosity (cP)	949.5	49.6	949.5
Asphalt Mixture			
WMA Mixture	M-B1	M-B2	M-B3
Aggregate majority (> 50%)	Gravel	Limestone	Gravel
Optimum binder content (%)	5.6	6.3	5.6
Dust/Binder Ratio	1.18	1.03	1.07

*Note: Mixtures with different binders were collected at 135±2 and 165±2 °C.

2.1.2 Asphalt Binder and Warm Mix Asphalt (WMA) additives

As can be seen in Table 2.1, one type of asphalt binder (PG 58H-34) was used in this study and obtained from two different sources (Flint hills and Jebro) depending on the site location.

The WMA additives employed in the plants were Evotherm® and Delta S®, and they were added to the asphalt binders at the dosage of 0.7% by the binder weight to increase the mixture workability, as well as to lower the production temperatures.

The Evotherm® composition is an emulsion of oil and water that reduces the viscosity of asphalt binder, whereas the water of emulsification flashes while in contact with the hot aggregates. This product recipe and ownership by the “Ingevity” company, is a cost-effective WMA additive with the potential of lowering the asphalt production temperatures by up to 30°C.

Delta S® is categorized as a true rejuvenator and an additive-based WMA technology. The product can return the binder of a recycled asphalt to its original functionality by reversing the natural oxidation process which is the main cause of pavement brittleness. Furthermore, Delta S® has the added benefit of acting as a WMA additive by reducing the mixing and compaction temperatures of asphalt mixtures. The product recipe is owned by the “Collaborative Aggregates” company.

2.2 Methods

2.2.1 Asphalt Binder Extraction Method

The first step in this experimental plan was to extract the binder from different asphalt mixtures following ASTM D2172 and D5404. To this end, three apparatus called Centrifuge, Reflux, and Rotavapor were utilized to wash reclaimed asphalt binder with solvent, filter the

washed binder, and extract binder from solvent, respectively. Figure 2.3 indicates three stages of the binder extraction method.

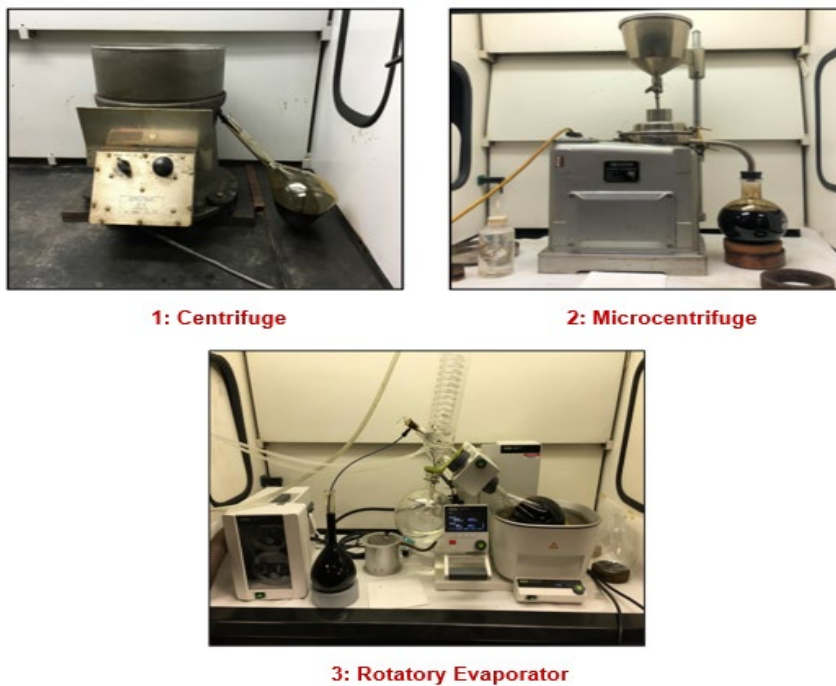


Figure 2.3 Asphalt binder extraction process stages

2.2.2 Standard Short-Term Aging (STA)

To simulate the effects of plant STA on asphalt mixtures, the standard RTFO procedure following ASTM D2872 was employed and applied to all types of asphalt binders. In accordance with this procedure, 35 g of asphalt binders inside cylindrical glass bottles are placed in a rotating carriage within an oven. The carriage rotates within the oven at a temperature of 163 °C to age the samples for 85 minutes. Furthermore, to investigate the effects of relevant parameters in the laboratory STA procedure as well as their potential interaction, various combinations of each parameter (time, temperature, airflow, and weight) are considered and adopted for this study. Further details are described in Section 2.5.

2.2.3 High-Temperature Performance Grade (PG)

To determine the high-temperature continuous PG of the binders, dynamic shear rheometer (DSR) tests were conducted following the AASHTO T315. The procedure made use of plates 25 mm in diameter at a 1-mm testing gap. Samples were attached to the DSR and subjected to pure shear tests to obtain the complex shear modulus (G^*) and phase angle (δ) of the studied binders. The test started at 52 °C and continued to 58, 64, and 70 °C with a frequency of 10 rad/sec in a sinusoidal waveform. The temperature at which the permanent deformation (rutting) parameter ($|G^*|/\sin\delta$) of short-term aged binders met the PG criterion, i.e., $|G^*|/\sin\delta > 2.2$ kPa was recorded as the continuous high-temperature PG of each binder. Different types of binders including extracted binders (short-term aged at 135 and 165 °C) and tank binders (unaged and RTFO aged) were tested for the high-temperature PG in this study. Figure 2.4 shows the DSR test setup for the high-temperature continuous PG test method.

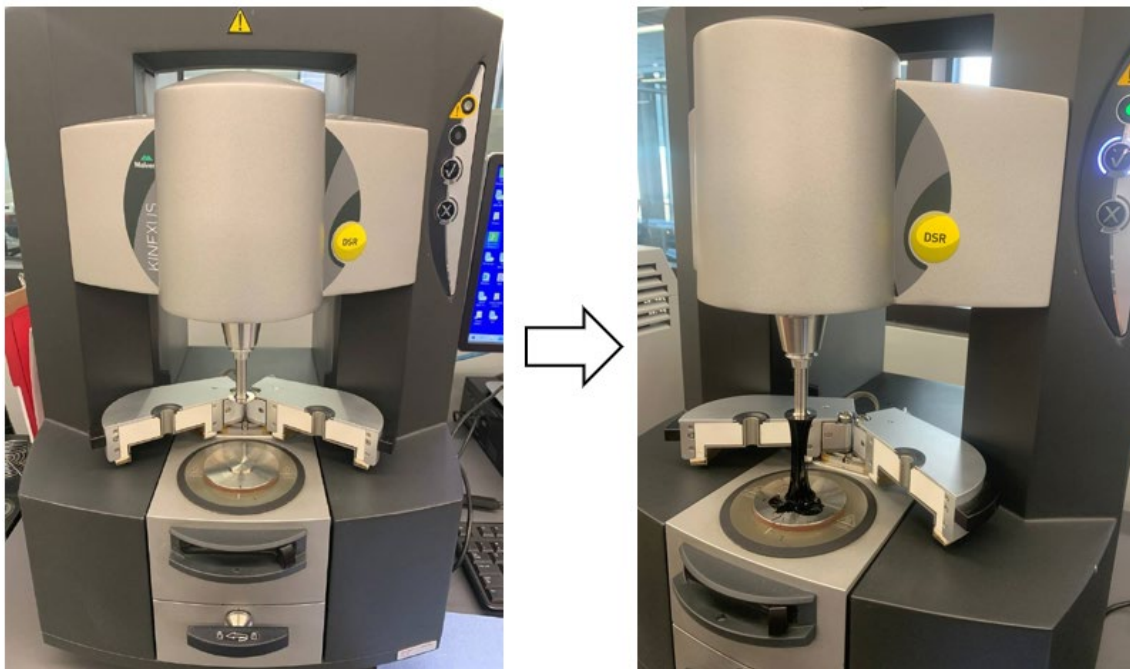


Figure 2.4 The DSR test setup for the High-temperature continuous PG measurement

2.2.4 Carbonyl Index Determination

To evaluate the aging condition of an asphalt binder, numerous studies rely on the determination of the carbonyl index (IC=O), obtained using the Fourier-transform infrared spectroscopy (FTIR) technique with the key wavenumber typically around 1700 cm^{-1} . The absorption spectrum is analyzed and the areas under the peaks are estimated. The FTIR test was conducted using a Nicolet Avatar 380 FTIR spectrometer based on the attenuated total reflection (ATR) mode. A resolution of 4 cm^{-1} within a wavenumber range of 400 to 4000 cm^{-1} was applied to record the spectra, while the OMNIC 8.1 software was further utilized to estimate the areas under the peaks. The FTIR test was conducted on both extracted binders (at 135 and $165\text{ }^{\circ}\text{C}$) and tank binders (unaged and RTFO aged) in this study. To evaluate the aging condition of an asphalt binder, carbonyl and sulfoxide indices are typically monitored, however, there are some reports about the limitations associated with sulfoxide index in terms of binder oxidation levels caused by aging [65], [66], [67]. Accordingly, IC=O, following Equation 1, was considered as the sole criterion to specify asphalt binder aging [68]. Figure 2.5 shows the FTIR setup and testing equipment for this study.

$$IC = O = \frac{\text{Area under } 1700\text{ cm}^{-1}\text{ peak}}{\text{Area under } 1400\text{--}1480\text{ cm}^{-1}\text{ peak}} \quad (1)$$

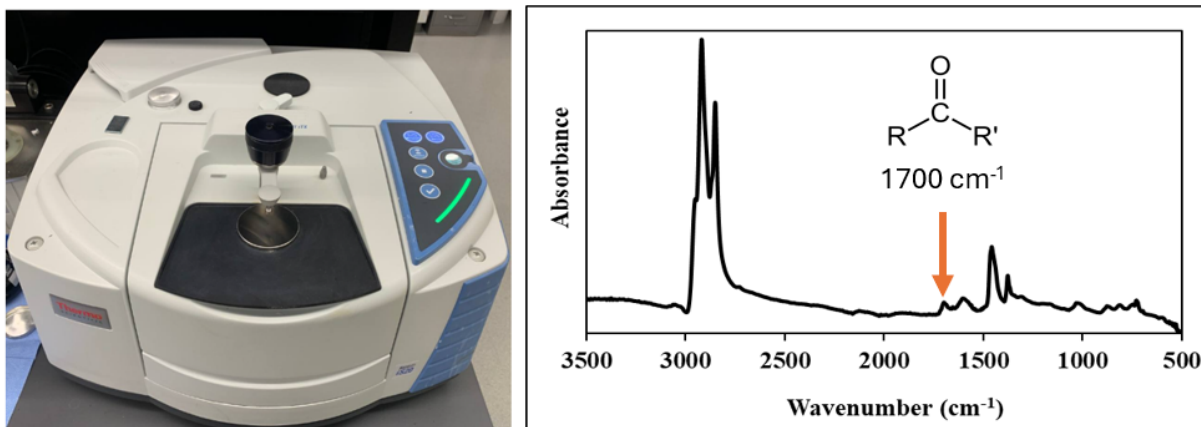


Figure 2.5 The FTIR test setup and equipment in this study

2.2.5 Elemental Analysis

To determine the oxygen content in the asphalt binders, a Thermo Finnigan FlashEATM Elemental Analyzer was utilized. The chromatographic column was then used to separate the resulting carbon monoxide, hydrogen, and nitrogen. Analyzing the carbon monoxide using FlashEA 1112, the oxygen percentage was obtained. Afterward, the sulfur dioxide derived from the binder sample combustion reaction was analyzed by a SC-632 sulfur determinator to obtain the sulfur part of the asphalt binder. Finally, the carbon, hydrogen, and nitrogen (CHN) amounts were measured by burning the samples in a pure oxygen atmosphere. Accordingly, the PerkinElmer 2400 series II CHNOS Analyzer has made use of the resulting combustion products (CO₂, H₂O, and N₂) to determine the elemental composition. The oxygen content was determined for both extracted binders (at 135 and 165 °C) and tank binders (unaged and RTFO aged) in this study.

2.3 Experimental Design Using Response Surface Methodology (RSM)

RSM is a statistical technique that offers significant benefits by optimizing processes and product designs through efficient exploration of input-output relationships. Design of

experiments using this method has found widespread application across diverse scientific and engineering disciplines [32, 69, 70, 71]. In this study, the RSM framework was adopted to establish a quantifiable relationship between the response variable and the control parameters. This relationship can subsequently be utilized to predict response values for various configurations of the control parameters. Using hypothesis testing methodologies, the statistical significance of the applied parameters can be determined and the optimal parameter settings that yield the desired response within a specified region of interest can be estimated.

As time, temperature, binder weight, airflow and their interactions are the main parameters considered in the RTFO protocol, the RSM method based on CDD in conjunction with multiple linear regression analysis was applied to evaluate the effects of these parameters on two main binder chemical and rheological responses: IC=O, and high-temperature PG. To facilitate the determination of model coefficients, three levels (high, medium, and low) were assumed for each parameter [72], considering literature review and engineering judgements. For instance, 135 °C was selected as the lower level of the temperature parameter to mimic the mixing and compaction of WMA mixtures in the field [4, 73], while 163 °C was the standard RTFO temperature. With that, the high-level temperature of 191 °C was selected using CDD requirements. Further, in the case of weight, the standard RTFO binder weight, 35 g, was selected as the highest level in this plan. 35 g was also reported as the amount of binder that could potentially creep out of the RTFO jar, especially, in modified binders with high viscosity [55]. With that in mind, 25 and 15 g were selected as the other two levels for binder weight parameter. The standard RTFO time of 85 minutes was selected as the middle time-parameter level. Forty-five minutes was selected as a suitable low level time for simulating aging in modified binders [32]. The airflow range was mainly selected based on the device capacity, with

the standard RTFO airflow rate (4 L/min) as the middle level. To predict the response variable across a range of input parameters, a quadratic polynomial regression model was adopted, as described in Equation 2:

$$Y = b_0 + \sum_{i=1}^k b_i x_i + \sum_{i=1}^k b_{ii} x_i^2 + \sum_{i=1}^{k-1} \sum_{j=i+1}^k b_{ij} x_i x_j \quad (2)$$

where Y = dependent response variable (i.e., IC=O and high-temperature PG); b_0 = intercept term; b_i , b_{ii} , and b_{ij} = measures of the effect of variable x_i , x_j , and $x_i x_j$, respectively, where x_i and x_j represent the independent parameters; and k = number of these parameters.

Chapter 3 Results and Discussion

In this chapter the results for asphalt binder characterization using standard RTFO protocol as well as different alternative protocols are presented. Accordingly, the standard RTFO results for unaged, plant aged (at two production temperatures), and laboratory aged binders are evaluated to determine the efficiency and accuracy of standard RTFO protocols for categorizing WMA binders. Following that, the results of using different combinations of RTFO parameters are analyzed to assess the interacting effects of these parameters on STA and to find out the appropriate aging protocol for simulating STA of WMA binders in the laboratory.

3.1 Asphalt Binder Characterization Based on Standard RTFO Protocol

The high-temperature PG and IC=O results for the unaged binders, extracted and recovered binders from plant-produced mixtures (produced at temperatures of 135 and 165 °C), and RTFO aged binders are represented in Figure 3.1. As mentioned in the previous chapter, two different scenarios were considered: the first scenario produced WMA mixtures at 135 °C to compare a lower temperature to the HMA production temperature; and the second scenario used WMA additives only as a compaction aid and produced the WMA mixture at a temperature of 165 °C. The results obtained from both scenarios of plant STA binders were considered to be separate target values for the laboratory aged binders to further optimize the input parameters for each scenario. Figure 3.1a shows that the high-temperature PG of RTFO-aged binders was higher than that of plant-aged binders at either production temperature, indicating that the standard RTFO aging protocol is severe for WMA binders. In the case of B1, the high-temperature PG for laboratory aged binder obtained from the standard RTFO procedure is 2.4 and 1.1 °C higher than that of plant-aged binders produced at 135 and 165 °C, respectively. The same comparison for B2 shows 2.9 and 1.7 °C higher PG values for laboratory-aged binders

compared to the plant-aged binders at 135 and 165 °C, respectively. This discrepancy between laboratory-aged protocol and plant-aged binders is further confirmed by the IC=O results, as shown in Figure 3.1b.

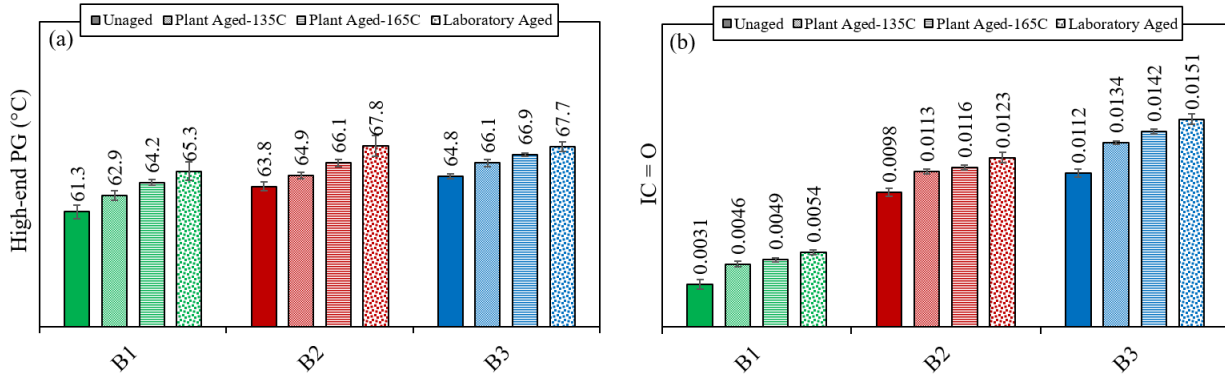


Figure 3.1 Properties of unaged, plant aged (135 and 165 °C), and laboratory aged binders (a) high-temperature PG and (b) IC=O

3.2 Effects of RTFO Parameters on Binder Properties

Using RSM methodology, and considering Equation 2, with $k = 4$ (time, temperature, airflow, binder weight), and a variable set at three levels (low, medium, high), 25 different combinations out of 81 possible cases (Table 3.1) were generated. The B1 and B2 binder samples were short-term aged using these different combinations of parameters inside the RTFO equipment, and all the samples were further tested for the main responses (IC=O and high-temperature PG) using three replicates. This procedure was conducted in a randomized order to avoid systematic bias. The final average response values are shown in Table 3.1.

Table 3.1 Input parameter arrangement and response values for laboratory-aged asphalt binders

Operational aging parameters					Parameter Response			
					High-temperature PG (°C)		IC=O	
Runs	Time (min)	Temperature (°C)	Weight (gr)	Airflow (L/min)	B1	B2	B1	B2
1	45	135	15	3	60.5	60.5	0.0016	0.0097
2	125	135	15	3	62.9	66.4	0.0018	0.0103
3	45	191	15	3	68.3	74.3	0.0077	0.0112
4	125	191	15	3	85.9	95.8	0.0247	0.0151
5	45	135	15	5	60.5	61.3	0.0011	0.0104
6	125	135	15	5	63.3	65.7	0.0013	0.0117
7	45	191	15	5	69.7	77.5	0.0100	0.0121
8	125	191	15	5	85.2	100.9	0.0240	0.0156
9	45	135	35	3	60.1	61.3	0.0013	0.0102
10	125	135	35	3	62.3	63.7	0.0007	0.0117
11	45	191	35	3	64.1	66.7	0.0028	0.0105
12	125	191	35	3	72.3	80.4	0.0131	0.0136
13	45	135	35	5	60.3	61.3	0.0025	0.0104
14	125	135	35	5	62.4	65.1	0.0004	0.0106
15	45	191	35	5	63.2	66.7	0.0031	0.0109
16	125	191	35	5	72.2	81.9	0.0138	0.0137
17	45	163	25	4	63.4	65.8	0.0015	0.0112
18	125	163	25	4	68.6	74.7	0.0094	0.0118
19	85	135	25	4	61.9	63.5	0.0011	0.0115
20	85	191	25	4	72.1	81.0	0.0143	0.0122
21	85	163	25	3	66.3	70.6	0.0062	0.0115
22	85	163	25	5	66.5	70.8	0.0054	0.0116
23	85	163	15	4	67.1	72.8	0.0069	0.0122
24	85	163	35	4	65.3	67.8	0.0054	0.0123
25	85	163	25	4	65.5	69.4	0.0149	0.0119

3.3 Model Fitting

The analysis of variance (ANOVA) was performed on the responses (high-temperature PG and IC=O) considering a confidence level of 90% ($\alpha = 0.1$). The p-values lower than 0.1 are associated with parameters that have significant effects on responses. Table 3.2 presents the ANOVA results. From Table 3.2, it can be seen that the first order (linear) terms of time,

temperature, and weight have significant effects on high-temperature PG and IC=O values of both binders (B1 and B2). The airflow effect (in the range selected for this study) was found to be insignificant in all cases, except for the high-temperature PG of B2 in which the p-value was found to be lower than 0.1. Even in this case, the contribution of the input parameter was found to be less than 0.3%. Furthermore, the interactive terms of time-temperature, temperature-weight, and time-weight are found to be statistically significant on the high-temperature PG and IC=O, within the studied range. The quadratic term of temperature is the only squared term which is found to be statistically significant in the case of high-temperature PG for B2 binder.

Table 3.2 ANOVA table for B1 and B2 binders: High-end PG and IC=O

Parameter term/Response	DF	High-temperature PG – B1			High-temperature PG – B2		
		Contribution (%)	P-value	Significant?	Contribution (%)	P-value	Significant?
Model	14	97.92	0.000	Yes	99.21	0.000	Yes
Linear	4	79.32	0.000	Yes	83.12	0.000	Yes
Time	1	21.37	0.000	Yes	21.46	0.000	Yes
Temperature	1	49.3	0.000	Yes	53.36	0.000	Yes
Weight	1	8.58	0.000	Yes	8.01	0.000	Yes
Airflow	1	0.00	0.927	No	0.29	0.085	Yes
Square	4	0.45	0.710	No	0.56	0.209	No
Time × Time	1	0.00	0.885	No	0.00	0.830	No
Temp. × Temp.	1	0.17	0.385	No	0.33	0.070	Yes
Weight × Weight	1	0.00	0.951	No	0.00	0.746	No
Airflow × Airflow	1	0.00	0.790	No	0.00	0.781	No
2-Way Interaction	6	18.16	0.000	Yes	15.53	0.000	Yes
Time × Temp.	1	9.47	0.000	Yes	8.06	0.000	Yes
Time × Weight	1	1.61	0.019	Yes	0.99	0.005	Yes
Time × Airflow	1	0.00	0.872	No	0.00	0.574	No
Temp. × Weight	1	7.05	0.000	Yes	6.21	0.000	Yes

Parameter term/Response	DF	Contribution (%)	P-value	Significant?	Contribution (%)	P-value	Significant?
		High-temperature PG – B1			High-temperature PG – B2		
Temp. × Airflow	1	0.00	0.872	No	0.17	0.174	No
Airflow × Weight	1	0.02	0.772	No	0.07	0.355	No
Error	10	2.08	-	-	0.79	-	-
Total	24	100.00	-	-	100.00	-	-
		IC=O – B1			IC=O – B2		
Model	14	93.56	0.000	Yes	94	0.000	Yes
Linear	4	70.42	0.000	Yes	76	0.000	Yes
Time	1	15.76	0.001	Yes	34	0.000	Yes
Temperature	1	48.56	0.000	Yes	38	0.000	Yes
Weight	1	6.10	0.012	Yes	2	0.059	Yes
Airflow	1	0.00	0.891	No	2	0.176	No
Square	4	0.76	0.864	No	0	0.888	No
Time × Time	1	0.25	0.539	No	0	0.570	No
Temp. × Temp.	1	0.34	0.507	No	0	0.732	No
Weight × Weight	1	0.00	0.837	No	0	0.463	No
Airflow × Airflow	1	0.08	0.689	No	0	0.573	No
2-Way Interaction	6	22.29	0.008	Yes	20	0.010	Yes
Time × Temp.	1	15.59	0.001	Yes	12	0.001	Yes
Time × Weight	1	0.93	0.263	No	0	0.396	No
Time × Airflow	1	0.08	0.728	No	0	0.545	No
Temp. × Weight	1	5.68	0.014	Yes	4	0.016	Yes
Temp. × Airflow	1	0.00	0.806	No	0	0.728	No
Airflow × Weight	1	0.00	0.912	No	2	0.103	No
Error	10	6.44	-	-	6	-	-
Total	24	100	-	-	100	-	-

Overall, using the calculated regression coefficients, four polynomial statistical models are developed for each studied response, as shown in Equations 3 to 6, with R-squared values of 97.9, 99.2, 93.6, and 94.2%, respectively.

$$\text{High-temperature PG (B1)} = 55.9 - 0.194\text{time} - 0.149\text{Temp.} + 1.290\text{Weight} + 0.002277\text{time} \times \text{Temp.} - 0.002625\text{time} \times \text{Weight} - 0.00786\text{Temp.} \times \text{Weight} \quad (3)$$

$$\text{High-temperature PG (B2)} = 78.6 - 0.305\text{time} - 0.505\text{Temp.} + 2.046\text{Weight} - 3.99\text{Airflow} + 0.00230\text{Temp.}^2 + 0.003198\text{time} \times \text{Temp.} - 0.003141\text{time} \times \text{Weight} - 0.01123\text{Temp.} \times \text{Weight} \quad (4)$$

$$\text{IC=O (B1)} = 0.0051 - 0.000221\text{time} - 0.000393\text{Temp.} + 0.00131\text{Weight} + 0.000003\text{time} \times \text{Temp.} - 0.000002\text{time} \times \text{Weight} - 0.000007\text{Temp.} \times \text{Weight} \quad (5)$$

$$\text{IC=O (B2)} = 0.0044 - 0.000026\text{time} - 0.000031\text{Temp.} + 0.000193\text{Weight} + 0.000001\text{time} \times \text{Temp.} - 0.000000\text{time} \times \text{Weight} - 0.000001\text{Temp.} \times \text{Weight} \quad (6)$$

The graphical representation of those models for the binder B2 is exemplified in Figure 3.2. Similar trends were obtained for binder B1. In each graph, the interactive effects of two parameters were plotted, while the other two parameters were kept constant on their middle level. As seen, the parallel lines in each case implied that the interaction did not affect the relationship between the factors and response. For instance, the relationship between airflow and other factors in the case of high-temperature PG (Figure 3.2b) showed no interaction effect. In some cases of IC=O (Figure 3.2a), the airflow shows some interaction effects, however, the ANOVA test results presented in Table 3.2 confirm that these effects were statistically insignificant. This insignificant effect of airflow in the selected range of this study might be related to the fixed speed of RTFO carriage. The carriage speed might need to be adjusted in accordance with the airflow rate to further check the effect of airflow on the responses [32].

Further, there might be a need to extend the range of airflow (beyond 3 to 5 L/min) for future studies to capture some effects from this parameter.

The non-parallel lines indicate the interaction effect was meaningful, with a greater differences in line slopes showing stronger interaction effects. For instance, time, temperature, and weight showed individual and interactive effects on both responses, with the ANOVA results confirming the significance of these effects. As seen in Figure 3.2a and b, increasing the binder weight while keeping time and temperature constant lowered the high-temperature PG and IC=O of binders. According to literature, 35 g of binder in a standard RTFO procedure can form a film thickness of 1.25 mm inside the bottle, while decreasing the weight to 15 mm reduces the film thickness to around 0.54 mm and leads to a facile diffusivity of oxygen through the binder and intensifying the aging effects [74].

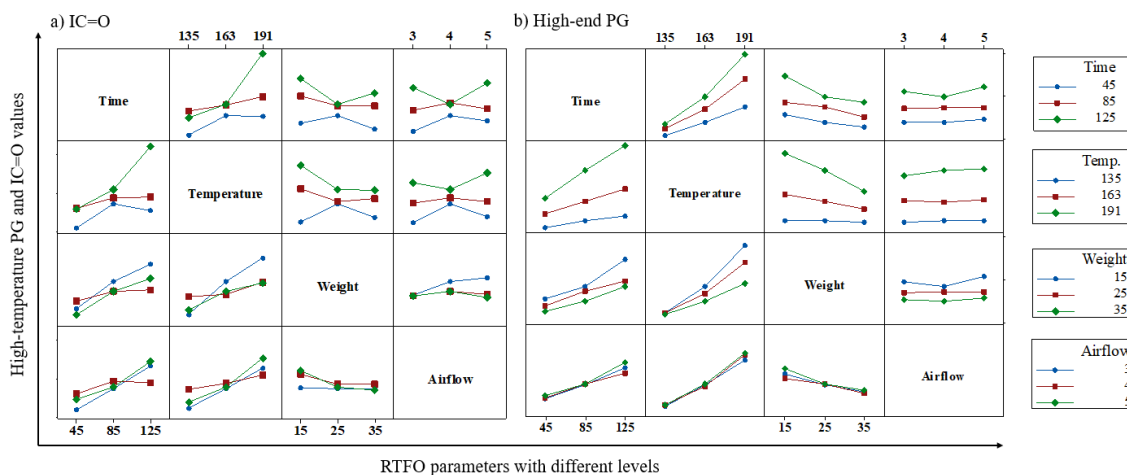


Figure 3.2 Interaction plots of RTFO parameters for B2: (a) IC=O and (b) high-temperature PG

3.4 Proposed Modified RTFO Protocol

Different combinations of aging parameters within the studied range could be selected that result in a short-term aged binder similar to what occurs in the plant for WMA binders (target values from extracted plant STA binders). The relative effects of parameters on the responses are examined thorough contour plots as shown in Figure 3.3 (a-d).

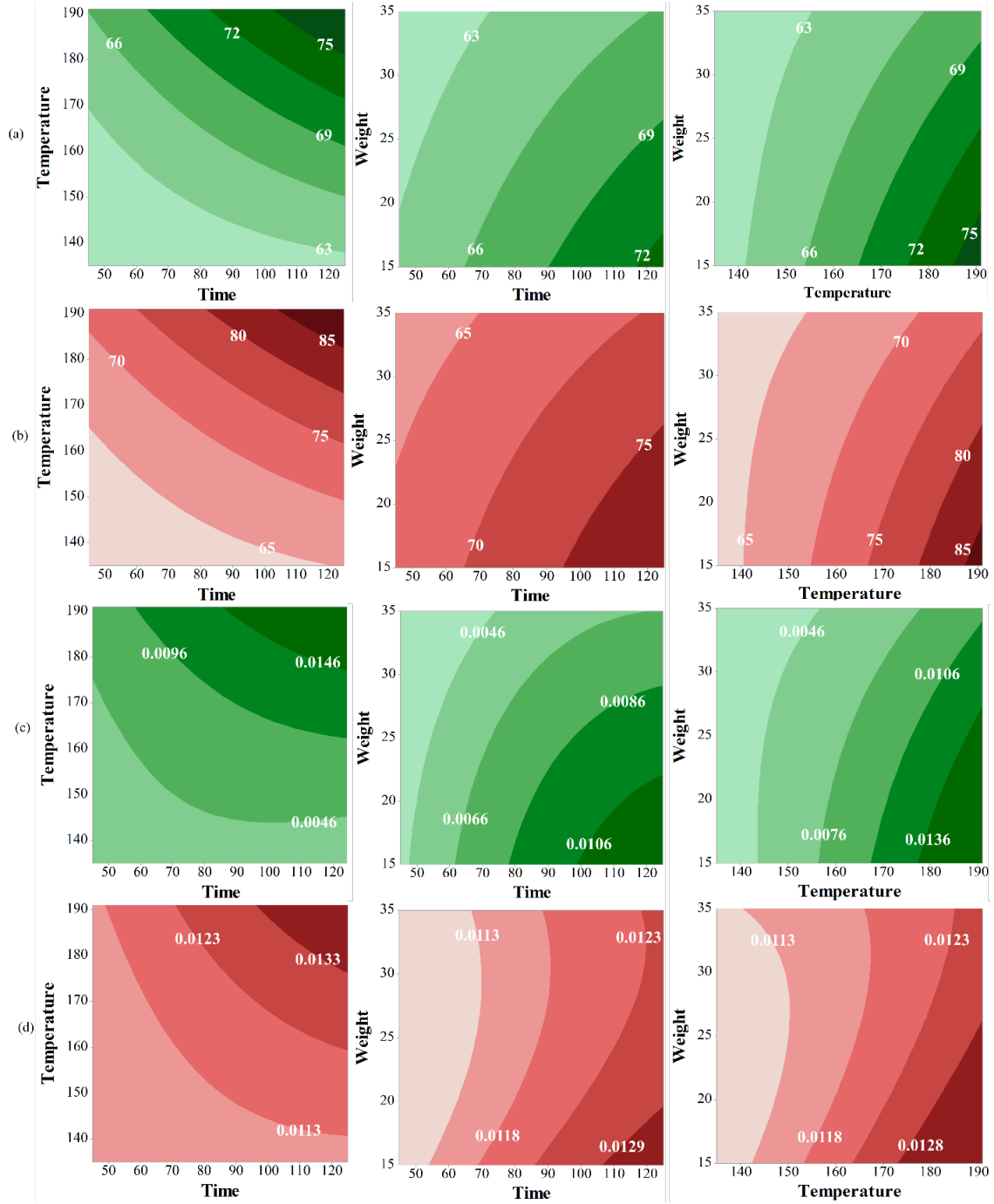


Figure 3.3 Contour plots: (a) high-temperature PG of B1, (b) high-temperature PG of B2, (c) IC=O of B1, and (d) IC=O of B2

For the first scenario, the target values are selected from field STA binders that are produced at 135 °C, as a common temperature for WMA production. Accordingly, any point on

the curves of 63 and 65 in Figure 3.3a and b results in the corresponding target PG of the same binder produced at 135 °C. To ensure that the chemical properties of binders are also similar to those aged in the plant, the same procedure has been done for the IC=O target values from B1 and B2 (Figure 3.3c and d). Several combinations of input parameters could be derived from this method. Some examples considering engineering judgements, and some test limitations are shown in Table 3.3.

Table 3.3 Combination of parameters as alternative RTFO protocol for WMA binders produced at 135 °C (first scenario)

Alternative	Time (min)	Temperature (°C)	Weight (gr)
Based on High-temperature PG of B1			
1	45	168	25
2	72	163	35
3	85	146	25
Based on High-temperature PG of B2			
1	45	165	25
2	70	163	35
3	85	143	25
Based on IC=O of B1			
1	45	175	25
2	73	163	35
3	85	145	25
Based on IC=O of B2			
1	50	188	25
2	69	163	35
3	85	150	25

As can be seen, extreme conditions, especially elevated temperatures are inhibited in the selected combinations. The reason is mainly due to the formation of carboxylic anhydrides and some other highly oxidized species under severe aging conditions which can lead to some levels of binder hardening that do not occur in the field aging process [75]. These different

combinations of parameters can be used to simulate short-term aging of WMA binders within the range of this study. Among them, the following conditions are selected as a common combination among both types of binders and both responses:

Suggested Modified RTFO parameters (scenario 1):

Time = 70 min, temperature = 163 °C, weight = 35 gr, and airflow = 4 L/min.

The proposed parameters for the modified RTFO were very similar to the standard RTFO protocol, except that the time had been reduced from 85 minutes to 70 minutes. The temperature remained at 163 °C, as the higher temperatures could have potentially changed some chemical properties of asphalt binders rather than IC=O. An alternative method could be selected with shorter time and 25 g of binders. The shorter period could save some time and lower binder content could avoid spilling issues while rotating the RTFO carriage. However, aging 25 g of binder means there would be a need for three bottles of RTFO aged binder to produce enough binder for a PAV pan (rather than two bottles when using 35 g of binder). This could turn into a potential concern for the quality control production laboratories since with the standard protocol, four types of binders can be aged thorough one RTFO cycle, while only two binder types can be aged using a protocol with 25 g of binder.

For the second scenario, the target values were selected from field STA binders produced at 165 °C, a typical temperature for producing HMA. In this scenario, the WMA additives might serve as compaction aids to lower the viscosity of loose mixtures, as is the case for the state of Nebraska. Using the same contour plots as shown in Figure 3.3, any points on the curves of 64.2 and 66 in Figure 3.3a and b resulted in the corresponding PG of the B1 and B2, respectively. The same procedure was applied for the curves of 0.0049 and 0.0116 in Figure 3.3c and d, representing target IC=O of B1 and B2, respectively. From several combinations of input

parameters that could be derived from this method, the following conditions were selected as a common combination among both types of binders and both responses:

Suggested Modified RTFO parameters (scenario 2):

Time = 85 min, temperature = 150 °C, weight = 25 gr, and airflow = 4 L/min.

The proposed protocol for the modified RTFO in the second scenario kept the time of 85 minutes. The temperature reduced from 163 °C to 150 °C, which protected the binder from chemical changes due to temperature effects. The binder weight was reduced to 25 g, which is 10 g lower than the standard RTFO protocol. The concern remains for quality control production laboratories, in which only two types of binder can be aged using a protocol with 25 g of binder. However, this concern can be addressed by applying a new approach for determining low-temperature PG of asphalt binders. In this approach, 4-mm parallel plates on the DSR machine are adopted to find the low-temperature PG as a replacement for BBR test [76, 77]. With the acceptance of the 4-mm DSR process, one RTFO bottle would be sufficient to determine the low-temperature PG. However, another modification would be necessary to reduce the PAV pan diameter to assure the same level of aging in PAV for 20 hours.

3.5 Validation of the Modified RTFO Protocols

To examine the applicability of this proposed short-term aging protocol for WMA binders, characterization results from a third binder (B3) was used. The chemical and rheological properties of this laboratory-aged binder were compared to the plant short-term aged results (target values). Figure 3.4a presents the high-temperature PG and IC=O results for B3, aged under the modified RTFO protocol (first scenario), as well as standard RTFO, and field aged at 135 °C. With respect to high-temperature PG, an absolute difference value of 0.30% was observed between the modified protocol and plant-aged binder, while for the IC=O, the absolute

difference value was 2.98%. Comparing standard RTFO with plant aged binder showed an absolute difference of 2.42% for high-temperature PG and 12.69% for IC=O. Figure 3.4b shows the same comparison between modified RTFO (second scenario), standard RTFO, and field aged binder produced at 165 °C. Considering high-temperature PG, the absolute difference between modified RTFO and plant-aged is 0.15%, while the same comparison between standard RTFO and plant-aged shows an absolute difference of 1.3%. In the case of IC=O, the absolute difference between modified RTFO and plant-aged is 1.4%, and between standard RTFO and plant-aged is 6.3%. These results can be used as an indication for the capability of these proposed protocols to accurately simulate short-term aging of WMA binders, within the range of this study.

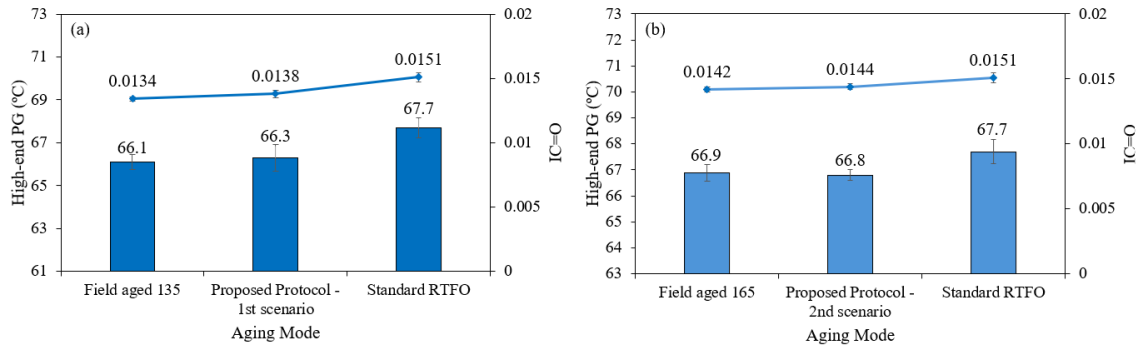


Figure 3.4 High-end PG and IC=O of B3 aged in the field, and with the current and proposed STA protocols: (a) first scenario and (b) second scenario

Chapter 4 Thermal Simulation

Asphalt pavements are essential infrastructure components that are subjected to severe thermal fluctuations throughout their lifetime. These thermal variations can affect the material properties, performance, and durability of the pavement [78]. Therefore, understanding the temperature distribution within the asphalt layer is crucial for optimizing various aspects of pavement design, construction, and long-term performance. Specifically, the temperature gradient within the asphalt mixture affects the potential cracking behavior, etc. Modeling the heat transfer behavior of asphalt pavement provides significant insight into its thermal performance. Numerical methods, such as the finite difference method (FDM), are commonly employed to predict temperature profiles within the pavement structure. These models enable engineers to project thermal behavior under real-world conditions, allowing for better-informed decisions during the design and maintenance of roadways. Asphalt pavements are composite materials composed of aggregates, asphalt binder, and air voids. The behavior of these components under thermal loads must be considered when simulating heat transfer mechanisms such as conduction and convection. Figure 4.1 illustrates the schematic of heat dissipation from an asphalt mixture control volume with a standard (pre-compaction) thickness of 63 mm. The asphalt mixture has an initial temperature of 176 °C and loses heat through conduction to the underlying ground at 25 °C and through convection to the ambient air. The finite difference method (FDM) was employed to discretize the control volume into N nodes and solve the governing heat transfer equations, capturing the conductive and convective heat transfer processes.

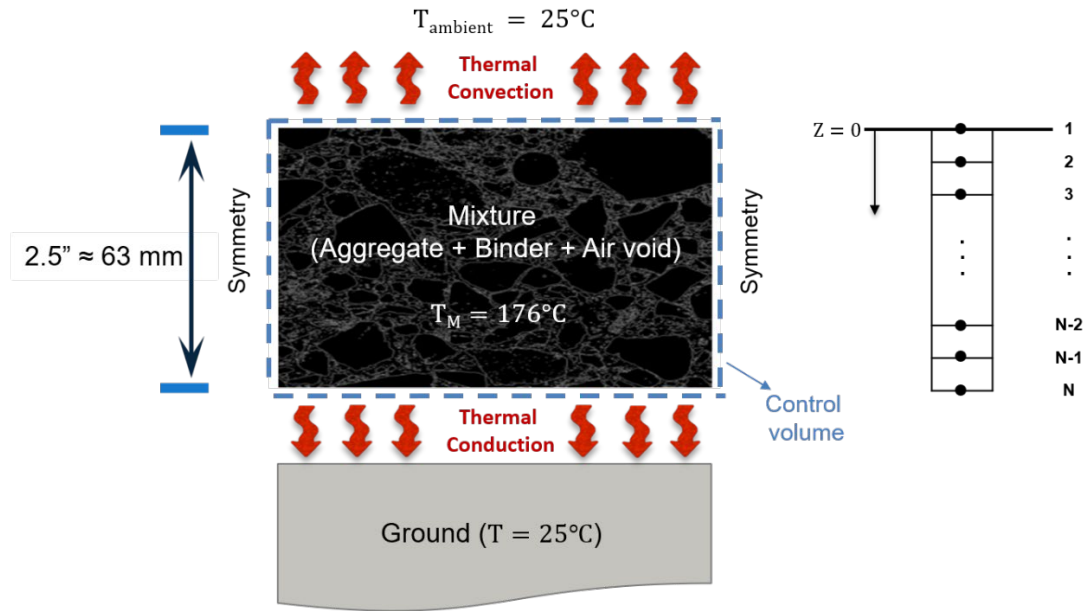


Figure 4.1 Schematic representation of heat dissipation from a 63 mm (pre-compression) asphalt mixture with an initial temperature of 176 °C.

This chapter focuses on thermal modeling and analysis of the asphalt mixture in its application on the roadway. The analysis incorporates the material's composite (aggregates, air voids, and binder) as well as the external boundary conditions (e.g., ambient air temperature, wind speed, etc.) that determine heat dissipation. By solving the governing heat transfer equations using FDM, the thermal profile can be mapped over time, providing insights into the heat transfer behavior of the mixture under transient thermal conditions.

The thickness of an asphalt layer, typically 50.8 mm (2 inches) for road pavements after compaction, is a critical factor in understanding its thermal behavior. Before compaction, this thickness is generally around 63.5 mm (2.5 inches), which forms the basis for the thermal simulations in this study. The material composition of asphalt pavements significantly affects heat transfer mechanisms. Asphalt compositions (aggregates, asphalt binder, and air voids), each contribute unique thermal and physical properties to the mixture.

Aggregates in the mixture vary widely in size, ranging from coarse stones (19.5 mm) to fine particles (75 μm). This size variation directly impacts the material's overall thermal conductivity and cooling behavior. The asphalt binder, which coats and binds the aggregates, has a thickness that ranges from 4 μm to 13 μm (considered in this study). The small size of the binder layer, combined with its relatively low thermal conductivity, makes it a key player in heat retention within the pavement structure. Additionally, the air void content of the mixture, 14% in this study, also influences the effective thermal properties and cooling rate.

To simulate the cooling process of the asphalt mixture after placement, a transient conduction heat transfer approach was used, modelling the time-dependent temperature distribution within the asphalt layer. The initial temperature of the mixture was set at 176 °C, reflecting typical temperatures during paving operations. Two boundary conditions were applied: the top boundary was exposed to ambient air, and the bottom boundary was in contact with the ground. Both ambient air and ground temperatures were assumed to remain constant at 25 °C.

The thermal and physical properties of the materials used in the asphalt mixture (aggregates, binder, air voids) and the underlying soil are critical for accurately modeling heat transfer. These properties, such as thermal conductivity, specific heat capacity, and density, were incorporated into the simulation and are summarized in Table 4.1.

Table 4.1 Thermal and physical properties of inclusion materials in asphalt mixture

properties	aggregate	binder	soil	air
Thermal				
conductivity, k (W/m.K)	1.7	0.25	0.8	0.026
Specific heat				
capacitance, c_p (kJ/kg. K)	0.9	1.2	1.1	1
Density, ρ (kg/m ³)	910	990	1400	1.29
Thermal diffusivity, α ($\mu\text{m}^2/\text{s}$)	1.4	2.04	0.5	20
Smallest size (μm)	75	4	-	-
Largest size	19.5 mm	13 μm	-	-

The thermal conductivity values reflect the different capabilities of each component to conduct heat, with the aggregates having the highest thermal conductivity (1.7 W/m·K) and air having the lowest (0.026 W/m·K). The specific heat capacity values indicate the amount of energy required to change the temperature of the materials, and the densities provide insight into how these materials store thermal energy. The thermal diffusivity, a key parameter for transient heat transfer, represents how quickly the material can conduct thermal energy relative to its capacity to store it. In addition to conduction, heat transfer due to convection at the surface was modeled using a wind speed of 7 m/s, which is representative of typical outdoor conditions during asphalt placement.

To model the thermal behavior of the asphalt layer, the FDM was employed. This numerical technique discretizes the asphalt mixture into small control volumes (nodes), as shown in Figure 4.1, allowing the governing heat transfer equations to be solved iteratively over time. The finite difference approach is particularly suited for transient heat transfer problems where the temperature distribution within a material changes over time. The governing heat transfer equation is expressed as Equation 7:

$$\frac{\partial T}{\partial t} = \alpha \nabla^2 T \quad (7)$$

where T is temperature, t is time, and α is the thermal diffusivity of the composite material. The term $\nabla^2 T$ represents the spatial variation of temperature, capturing how heat is conducted through the material. Using the weighted average approach for the thermal properties of the composite, the effective values for thermal conductivity, specific heat, and density were derived.

Focusing on the interplay between aggregate size and binder thickness, the simulation was implemented for three case studies, as described below:

- **Case 1:** The smallest possible aggregate sizes (75 μm).
- **Case 2:** The largest possible aggregate sizes (19.5 mm).
- **Case 3:** A mixture with aggregate sizes within 75 μm to 19.5 mm range.

Recognizing that real-world asphalt mixtures contain a variety of aggregate sizes, a standard normal distribution was employed to represent the probable aggregate sizes within the range of 75 μm to 19.5 mm. This distribution, illustrated in Figure 4.2, shows how aggregate sizes are distributed within the mixture. The x-axis represents the size of the aggregates, while the y-axis represents the probability density of each size. The curve in Figure 4.2 shows that most aggregates fall within a specific range, with fewer aggregates at the extremes of the size spectrum. Incorporating this distribution of aggregate sizes into the simulation modeled a more

realistic asphalt mixture, reflecting the variation in thermal properties due to size differences. This provided a more accurate prediction of the average cooling time for a typical asphalt mixture. Within each case, we further investigated the influence of two different binder thicknesses (4 μm and 13 μm).

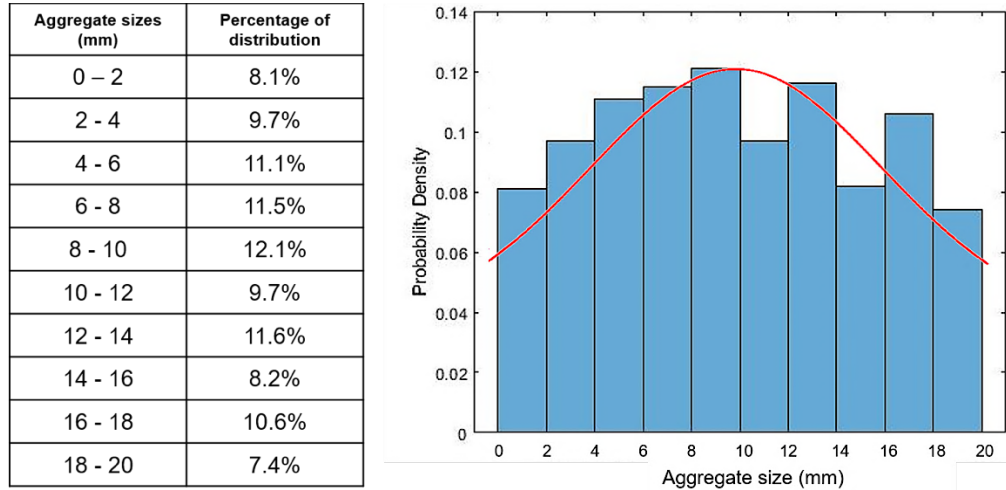


Figure 4.2 Illustration of the normal distribution of aggregate sizes within the asphalt mixture.

The simulation was performed under transient conditions, tracking the temperature drop from 176 °C to the critical compaction temperature of 135 °C. Figure 4.3 presents the thermal evolution of the asphalt layer for different aggregate sizes and binder thicknesses. The temperature was recorded over time at various depths within the asphalt mixture, providing insight into how heat dissipates through the layer as it approaches the critical temperature for compaction. As seen in Figure 4.3, for all three cases, the surface cooled down rapidly due to direct exposure to the surrounding environment, causing a steep temperature gradient near the top. However, the inner region (approximately -50 mm within the layer) of the asphalt layer exhibits a slower temperature drop, as heat is trapped within the thicker material. Moreover, the area near the ground cools faster than the inner region due to the lower ground temperature

(25 °C), which acts as a stable heat sink, enhancing heat conduction at the bottom. In the first scenario, the simulation considered the smallest aggregate size (75 μm) with binder thicknesses of 4 μm and 13 μm . This case represents the slowest cooling process among the three cases.

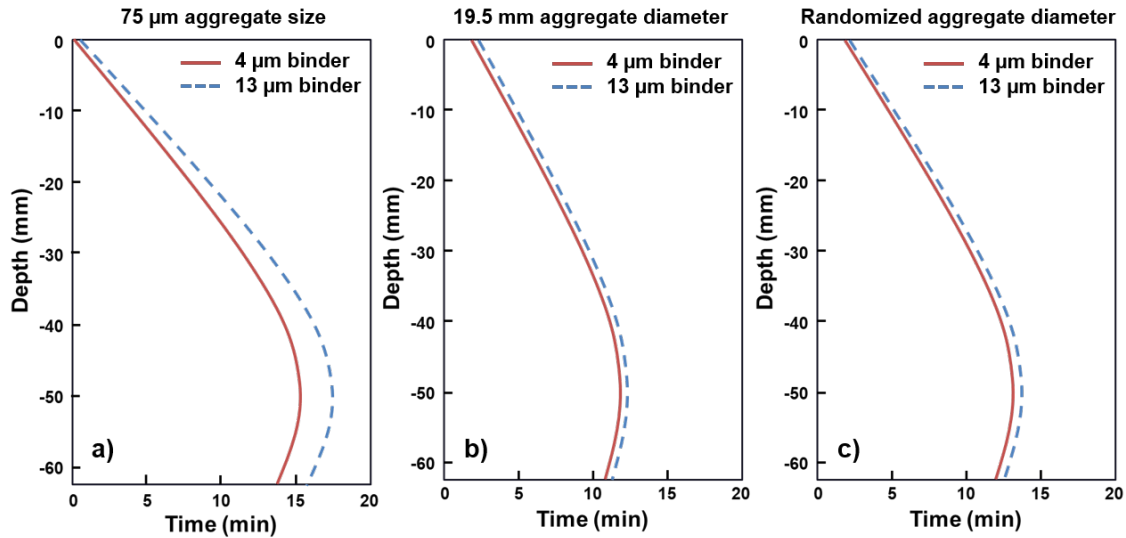


Figure 4.3 The time in which the mixture needs to reach $T = 135^{\circ}\text{C}$ after the application the roadway for (a) 75 μm aggregate with an average time of $\approx 11':45''$ and $\approx 13':05''$ for 4 μm and 13 μm binder, respectively, (b) 19.5 mm aggregate diameter with an average time of $\approx 9':52''$ and $\approx 10':40''$ for 4 μm and 13 μm binder, respectively, and (c) randomized aggregate sizes with an average time of $\approx 10':41''$ and $\approx 11':40''$ for 4 μm and 13 μm binder, respectively.

Figure 4.3a shows that the average time to reach 135°C is 11 minutes and 45 seconds when the binder is thinner (4 μm), while it takes 13 minutes and 5 seconds on average when the binder is thicker (13 μm). The last point within the control volume reaches 135°C within 15 minutes and 17 minutes for the compound with 4 μm and 13 μm binder thickness, respectively. In contrast, the second case modeled the largest aggregate size (19.5 mm) with similar binder thicknesses (Figure 4.3b). The heat transfer profile, in this case, is more uniform across the asphalt layer. The surface still cooled rapidly, but the middle layer experienced less resistance to heat flow compared to the smallest aggregate case. The larger aggregate size and reduced

interface resistance allowed for quicker heat dissipation throughout the entire layer. The bottom region near the ground cooled similarly to the first scenario due to the constant ground temperature. Still, overall, the larger aggregates reduced the duration for the entire asphalt layer to reach the critical temperature. In this case, the entire structure cooled uniformly within about 12 minutes and 13 minutes for the compound with 4 μm and 13 μm binder thickness, respectively. It is worth mentioning that, on average, it takes 9 minutes and 52 seconds and 10 minutes and 40 seconds for the mixture to reach 135 °C for the case with the thinner binder (4 μm) and thicker binder (13 μm), respectively. The result shows less difference between the different binder thicknesses for this case. The distributed aggregate size case offers a more representative case for practical applications, showing how a mixture of aggregate sizes can smooth out some of the variations in cooling time across the layer. The average time for the mixture with the thinner binder (4 μm) to cool to 135 °C was 10 minutes and 41 seconds, while with the thicker binder (13 μm) had an average time of 11 minutes and 40 seconds.

To further analyze the transient heat transfer, the temperature profile across the asphalt layer at the average cooling time for each case (smallest, largest, and distributed aggregate sizes) was simulated. The results are presented as three temperature-depth curves in Figure 4.4, showing how the temperature varies within the asphalt mixture at the average time that the mixture reaches the critical compaction temperature of 135 °C. In these graphs, the y-axis represents the depth from the surface of the asphalt layer to the ground (0 to 63 mm), while the x-axis shows the corresponding temperature at the average cooling times reported earlier. In each case, a vertical reference line marks the point where the temperature reaches 135 °C, highlighting the thermal behavior across the mixture depth.

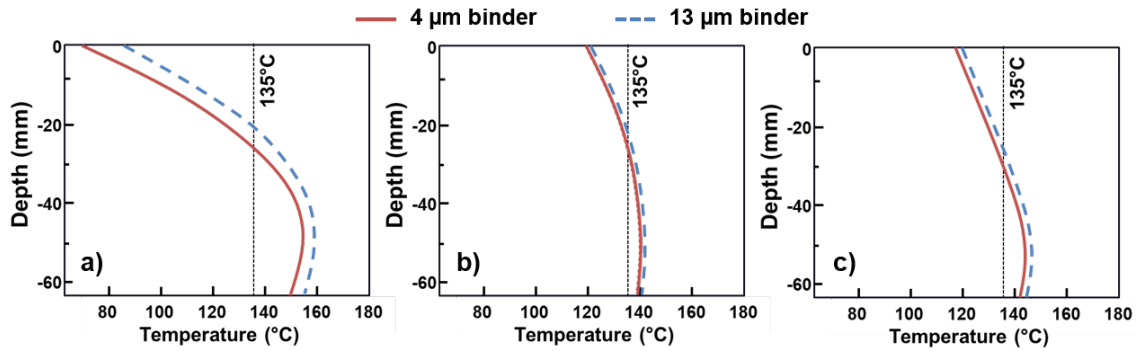


Figure 4.4 Temperature-depth profiles of asphalt layers. Each graph represents the temperature distribution at the specified time when the average temperature of the mixture reaches 135 °C. The solid line marks the vertical position of 135 °C, while the temperature at various depths demonstrates the cooling rate of each layer based on aggregate size (a) smallest aggregate, (b) largest aggregate, (c) distributed aggregate sizes.

The temperature gradient for the smallest aggregate case (75 μm) in Figure 4.4a shows a pronounced difference between the surface and deeper regions. Due to the fine aggregate size and its slower heat transfer rate, the temperature at the surface has reached 135 °C, while almost half of the layer of the depth remains above this temperature, indicating that the mixture is cooling unevenly. The steep slope seen in the plot suggests more thermal resistance within the smaller aggregate structure, as discussed earlier, potentially caused by increased interface resistance and surface area effects. In contrast, the largest aggregate scenario (19.5 mm) in Figure 4.4b presents a more uniform temperature distribution. At the surface level, the temperature has reached 135 °C, which drops rapidly with depth, indicating more effective heat conduction through the coarser structure. This result reinforces the hypothesis that larger aggregates, with fewer interface points and less overall surface area, provide a more efficient heat transfer pathway, allowing the entire layer to cool more evenly within a shorter timeframe. The distributed aggregate size case, shown in Figure 4.4c, falls between the two extremes regarding temperature distribution. While the temperature gradient is more gradual than that of

the largest aggregate case, it still exhibits a more balanced cooling behavior compared to the smallest aggregate.

These findings provide valuable insights for applying asphalt pavements. The data highlights the critical window of time available for effective compaction. By understanding the cooling behavior of the asphalt mixture, workers can ensure the application and compaction occur within the optimal temperature range, ultimately leading to a stronger and more durable pavement.

Chapter 5 Conclusions and Recommendation

This study employed RSM to investigate the short-term laboratory aging process of asphalt binders, focusing on two distinct WMA binders subjected to various combinations of aging parameters including time, temperature, airflow, and binder weight. The primary objectives were to enhance understanding of aging parameter efficacy and propose an alternative testing condition for the current laboratory short-term aging protocol that can simulate field aging in WMA binders. To validate the proposed protocol, a third asphalt binder underwent aging processes using it. The chemical and rheological properties of the aged binders were subsequently assessed using multiple analytical methods and results were compared to evaluate the efficacy of the new protocol. The following present key findings and conclusions derived from the test analyses:

- Statistical analysis revealed the significant effects of the first order of time, temperature, and weight, as well as their interactive terms on the major rheological and chemical responses from binders. However, the airflow rate's effect was found to be statistically insignificant within the studied range.
- A new protocol for laboratory short-term aging of WMA binders was developed to simulate field STA at 135 °C, featuring a reduced aging duration of 70 minutes at a temperature of 163 °C, utilizing 35 g of binder and an airflow rate of 4 L/min.
- A new protocol for laboratory short-term aging of WMA binders was developed to simulate field STA at 165 °C, featuring an aging duration of 85 minutes at the temperature of 150 °C, utilizing 25 g of binder and an airflow rate of 4 L/min.
- Comparative analysis demonstrated adequate consistency between the results of the field short-term aged binders and the proposed protocol, indicating the suitability and

applicability of the proposed method to simulate short-term aging of binders produced with WMA technology.

- The average allowable time window for compaction increases slightly by using smaller aggregates and a thicker binder layer surrounding aggregates. Using the critical window of time available for effective compaction ensures the compaction procedure being done within the optimal temperature range, ultimately leading to a stronger and more durable pavement.

For future research, a diverse selection of asphalt mixtures and binders with different aggregate sources and gradations and from different regions are targeted to further validate the proposed protocol. More than that, different chemical and rheological properties could be included as responses in the validation procedure including but not limited to low-temperature PG and Saturates, Aromatics, Resins, and Asphaltenes (SARA) analysis.

References

- [1] Mazumder, M., Sriraman, V., Kim, H. H., & Lee, S. J. (2016). Quantifying the environmental burdens of the hot mix asphalt (HMA) pavements and the production of warm mix asphalt (WMA). *International Journal of Pavement Research and Technology*, 9(3), 190-201.
- [2] Fast Facts. (2014). *Oncology Issues*, 29(4), 6–9.
- [3] Ameri, M., Afshin, A., Shiraz, M. E., & Yazdipناه, F. (2020). Effect of wax-based warm mix additives on fatigue and rutting performance of crumb rubber modified asphalt. *Construction and Building Materials*, 262, 120882.
- [4] Behnood, A. (2020). A review of the warm mix asphalt (WMA) technologies: Effects on thermo-mechanical and rheological properties. *Journal of Cleaner Production*, 259, 120817.
- [5] Diab, A., Sangiorgi, C., Ghabchi, R., Zaman, M., & Wahaballa, A. M. (2016). Warm mix asphalt (WMA) technologies: Benefits and drawbacks—A literature review. *Functional pavement design*, 1145-1154.
- [6] Hettiarachchi, C., Hou, X., Wang, J., & Xiao, F. (2019). A comprehensive review on the utilization of reclaimed asphalt material with warm mix asphalt technology. *Construction and Building Materials*, 227, 117096.
- [7] Almeida-Costa, A., & Benta, A. (2016). Economic and environmental impact study of warm mix asphalt compared to hot mix asphalt. *Journal of Cleaner Production*, 112, 2308-2317.
- [8] UN Framework Convention on Climate Change. (2015). Adoption of the Paris Agreement, *Conference of the Parties on its twenty-first session*, vol. 21932, no. December, p. 32.
- [9] Yousefi, A. A., Sobhi, S., Aliha, M. M., Pirmohammad, S., & Haghshenas, H. F. (2021). Cracking properties of warm mix asphalts containing reclaimed asphalt pavement and recycling agents under different loading modes. *Construction and Building Materials*, 300, 124130.
- [10] Yazdipناه, F., Ameri, M., Shahri, M., Hasheminejad, N., & Haghshenas, H. F. (2021). Laboratory investigation and statistical analysis of the rutting and fatigue resistance of asphalt mixtures containing crumb-rubber and wax-based warm mix asphalt additive. *Construction and Building Materials*, 309, 125165.
- [11] Kim, Y. R., Zhang, J., & Ban, H. (2012). Implementation of warm-mix asphalt mixtures in Nebraska pavements.
- [12] Bower, N., Wen, H., Wu, S., Willoughby, K., Weston, J., & DeVol, J. (2016). Evaluation of the performance of warm mix asphalt in Washington state. *International Journal of Pavement Engineering*, 17(5), 423-434.

- [13] Yang, X., You, Z., Perram, D., Hand, D., Ahmed, Z., Wei, W., & Luo, S. (2019). Emission analysis of recycled tire rubber modified asphalt in hot and warm mix conditions. *Journal of hazardous materials*, 365, 942-951.
- [14] Gandhi, T. (2008). *Effects of warm asphalt additives on asphalt binder and mixture properties* (Doctoral dissertation, Clemson University).
- [15] Gandhi, T. (2008). *Effects of warm asphalt additives on asphalt binder and mixture properties* (Doctoral dissertation, Clemson University).
- [16] Kumbarger, Y. S., & Biligiri, K. P. (2016). Understanding aging behaviour of conventional asphalt binders used in India. *Transportation Research Procedia*, 17, 282-290.
- [17] Sirin, O., Paul, D. K., & Kassem, E. (2018). State of the art study on aging of asphalt mixtures and use of antioxidant additives. *Advances in Civil Engineering*, 2018(1), 3428961.
- [18] Androjić, I. (2016). Ageing of hot mix asphalt. *Građevinar*, 68(06.), 477-483.
- [19] Bitumen, S. (1990). *The Shell bitumen handbook* (p. 232). Shell Bitumen UK.
- [20] Bell, C. A. (1989). *Summary report on aging of asphalt-aggregate systems* (Vol. 89, No. 4). Strategic Highway Research Program, National Research Council.
- [21] Petersen, J. C. (2009). A review of the fundamentals of asphalt oxidation: chemical, physicochemical, physical property, and durability relationships. *Transportation research circular*, (E-C140).
- [22] Masson, J. F., Collins, P., & Polomark, G. (2005). Steric hardening and the ordering of asphaltene in bitumen. *Energy & fuels*, 19(1), 120-122.
- [23] National Academies of Sciences, Engineering, and Medicine. (2021). Asphalt binder aging methods to accurately reflect mixture aging.
- [24] Camargo, I. G. D. N., Hofko, B., Mirwald, J., & Grothe, H. (2020). Effect of thermal and oxidative aging on asphalt binders rheology and chemical composition. *Materials*, 13(19), 4438.
- [25] Hou, X., Xiao, F., Wang, J., & Amirkhanian, S. (2018). Identification of asphalt aging characterization by spectrophotometry technique. *Fuel*, 226, 230-239.
- [26] Jing, R., Varveri, A., Liu, X., Scarpas, A., & Erkens, S. (2020). Rheological, fatigue and relaxation properties of aged bitumen. *International journal of pavement engineering*, 21(8), 1024-1033.
- [27] Zhang, H., Chen, Z., Xu, G., & Shi, C. (2018). Evaluation of aging behaviors of asphalt binders through different rheological indices. *Fuel*, 221, 78-88.

- [28] Abdullah, M. E., Zamhari, K. A., Buhari, R., Nayan, M. N., & Hainin, M. R. (2014). Short term and long term aging effects of asphalt binder modified with montmorillonite. *Key Engineering Materials*, 594, 996-1002.
- [29] Airey, G. D. (2003). State of the art report on ageing test methods for bituminous pavement materials. *International Journal of Pavement Engineering*, 4(3), 165-176.
- [30] Airey, G. D. (2003). State of the art report on ageing test methods for bituminous pavement materials. *International Journal of Pavement Engineering*, 4(3), 165-176.
- [31] Wasiuddin, N. M., & Arafat, M. S. (2018). *Development of a RTFO-Aging Test Protocol for WMA Binders and Its PG Grading* (No. SPTC15. 1-28). Southern Plains Transportation Center.
- [32] Haghshenas, H. F., Rea, R., Byre, D., Haghshenas, D. F., Reinke, G., & Zaumanis, M. (2020). Asphalt binder laboratory short-term aging: Effective parameters and new protocol for testing. *Journal of Materials in Civil Engineering*, 32(1), 04019327.
- [33] Arafat, S., & Wasiuddin, N. M. (2019). Understanding the short-term aging of warm mix asphalt using rolling thin film oven. *International Journal of Pavement Research and Technology*, 12, 638-647.
- [34] Shalaby, A. (2002). Modelling short-term aging of asphalt binders using the rolling thin film oven test. *Canadian Journal of Civil Engineering*, 29(1), 135-144.
- [35] Zhang, W., Bahadori, A., Shen, S., Wu, S., Muhunthan, B., & Mohammad, L. (2018). Comparison of laboratory and field asphalt aging for polymer-modified and warm-mix asphalt binders. *Journal of Materials in Civil Engineering*, 30(7), 04018150.
- [36] Veeraiah, H. K., & Nagabhushanarao, S. S. (2020). Effect of optimized short-term aging temperature on rheological properties of rubberized binders containing warm mix additives. *Construction and Building Materials*, 261, 120019.
- [37] Farrar, M. J., Grimes, R. W., Sui, C., Planche, J. P., Huang, S. C., Turner, T. F., & Glaser, R. (2012, June). Thin film oxidative aging and low temperature performance grading using small plate dynamic shear rheometry: An alternative to standard RTFO, PAV, and BBR. In *Proc., 5th Eurasphalt and Eurobitume Congress. Brussels, Belgium: Foundation Eurasphalt*.
- [38] Bahia, H. U., Zhai, H., & Rangel, A. (1998). Evaluation of stability, nature of modifier, and short-term aging of modified binders using new tests: LAST, PAT, and modified RTFO. *Transportation Research Record*, 1638(1), 64-71.
- [39] Federal Highway Administration, "The Universal Simple Aging Test," *FHWA TechBrief, Publication No. FHWA-HRT-15-054*, 2016.

- [40] Haghshenas, H. F., Rea, R., Byre, D., Haghshenas, D. F., Reinke, G., & Zaumanis, M. (2020). Asphalt binder laboratory short-term aging: Effective parameters and new protocol for testing. *Journal of Materials in Civil Engineering*, 32(1), 04019327.
- [41] Arafat, S., & Wasiuddin, N. M. (2019). Understanding the short-term aging of warm mix asphalt using rolling thin film oven. *International Journal of Pavement Research and Technology*, 12, 638-647.
- [42] Zhang, W., Bahadori, A., Shen, S., Wu, S., Muhunthan, B., & Mohammad, L. (2018). Comparison of laboratory and field asphalt aging for polymer-modified and warm-mix asphalt binders. *Journal of Materials in Civil Engineering*, 30(7), 04018150.
- [43] Ferrotti, G., Baaj, H., Besamusca, J., Bocci, M., Cannone-Falchetto, A., Grenfell, J., ... & You, Z. (2018). Comparison between bitumen aged in laboratory and recovered from HMA and WMA lab mixtures. *Materials and Structures*, 51, 1-13.
- [44] Hofko, B., Cannone Falchetto, A., Grenfell, J., Huber, L., Lu, X., Porot, L., ... & You, Z. (2017). Effect of short-term ageing temperature on bitumen properties. *Road Materials and Pavement Design*, 18(sup2), 108-117.
- [45] Yazdipناه, F., Khedmati, M., & Haghshenas, H. F. (2023). *Nebraska Balanced Mix Design-Phase I* (No. SPR-FY22 (002)). Nebraska. Department of Transportation.
- [46] Yin, F., & West, R. C. (2021). *Balanced mix design resource guide* (No. IS-143).
- [47] Abbas, A. R., Nazzal, M., Kaya, S., Akinbowale, S., Subedi, B., Arefin, M. S., & Abu Qtaish, L. (2016). Effect of aging on foamed warm mix asphalt produced by water injection. *Journal of Materials in Civil Engineering*, 28(11), 04016128.
- [48] Xiao, F., Punith, V. S., & Putman, B. J. (2013). Effect of compaction temperature on rutting and moisture resistance of foamed warm-mix-asphalt mixtures. *Journal of materials in civil engineering*, 25(9), 1344-1352.
- [49] Malladi, H., Ayyala, D., Tayebali, A. A., & Khosla, N. P. (2015). Laboratory evaluation of warm-mix asphalt mixtures for moisture and rutting susceptibility. *Journal of Materials in Civil Engineering*, 27(5), 04014162.
- [50] Behnood, A., Karimi, M. M., & Cheraghian, G. (2020). Coupled effects of warm mix asphalt (WMA) additives and rheological modifiers on the properties of asphalt binders. *Cleaner Engineering and Technology*, 1, 100028.
- [51] Ameri, M., Yazdipناه, F., Rahimi Yengejeh, A., & Afshin, A. (2020). Production temperatures and mechanical performance of rubberized asphalt mixtures modified with two warm mix asphalt (WMA) additives. *Materials and Structures*, 53, 1-16.
- [52] Yazdipناه, F., Ameri, M., Shahri, M., Hasheminejad, N., & Haghshenas, H. F. (2021). Laboratory investigation and statistical analysis of the rutting and fatigue resistance of

- asphalt mixtures containing crumb-rubber and wax-based warm mix asphalt additive. *Construction and Building Materials*, 309, 125165.
- [53] Omranian, S. R., Hamzah, M. O., Yee, T. S., & Mohd Hasan, M. R. (2020). Effects of short-term ageing scenarios on asphalt mixtures' fracture properties using imaging technique and response surface method. *International Journal of Pavement Engineering*, 21(11), 1374-1392.
- [54] Omranian, S. R., Hamzah, M. O., Valentin, J., & Hasan, M. R. M. (2018). Determination of optimal mix from the standpoint of short term aging based on asphalt mixture fracture properties using response surface method. *Construction and Building Materials*, 179, 35-48.
- [55] Design, S. M. Characterization of Modified Asphalt Binders in Superpave Mix Design.
- [56] Farrar, M. J., Grimes, R. W., Sui, C., Planche, J. P., Huang, S. C., Turner, T. F., & Glaser, R. (2012, June). Thin film oxidative aging and low temperature performance grading using small plate dynamic shear rheometry: An alternative to standard RTFO, PAV, and BBR. In *Proc., 5th Eurasphalt and Eurobitume Congress. Brussels, Belgium: Foundation Eurasphalt*.
- [57] Bahia, H. U., Hanson, D. I., Zeng, M., Zhai, H., Khatri, M. A., & Anderson, R. M. (2001). *Characterization of modified asphalt binders in superpave mix design* (No. Project 9-10 FY'96).
- [58] Ferrotti, G., Baaj, H., Besamusca, J., Bocci, M., Cannone-Falchetto, A., Grenfell, J., ... & You, Z. (2018). Comparison between bitumen aged in laboratory and recovered from HMA and WMA lab mixtures. *Materials and Structures*, 51, 1-13.
- [59] Veeraiah, H. K., & Nagabhushanarao, S. S. (2020). Effect of optimized short-term aging temperature on rheological properties of rubberized binders containing warm mix additives. *Construction and Building Materials*, 261, 120019.
- [60] Yener, E., & Himislioğlu, S. (2014). Effects of exposure time and temperature in aging test on asphalt binder properties. *International Journal of Civil & Structural Engineering*, 5(2), 112-124.
- [61] Lolly, R., Zeiada, W., Souliman, M., & Kaloush, K. (2018). Effects of short-term aging on asphalt binders and hot mix asphalt at elevated temperatures and extended aging time.
- [62] Khodaii, A., Mousavi, E. S., Khedmati, M., & Iranitalab, A. (2016). Identification of dominant parameters for stripping potential in warm mix asphalt using response surface methodology. *Materials and Structures*, 49, 2425-2437.
- [63] A Khodaii, A., Haghshenas, H. F., & Tehrani, H. K. (2012). Effect of grading and lime content on HMA stripping using statistical methodology. *Construction and Building Materials*, 34, 131-135.

- [64] Haghshenas, H. F., Khodaii, A., Hossain, M., & Gedafa, D. S. (2015). Stripping potential of HMA and SMA: A study using statistical approach. *Journal of materials in civil engineering*, 27(11), 06015002.
- [65] Abdullah, M. E., Zamhari, K. A., Buhari, R., Nayan, M. N., & Hainin, M. R. (2014). Short term and long term aging effects of asphalt binder modified with montmorillonite. *Key Engineering Materials*, 594, 996-1002.
- [66] Xu, G., Wang, H., & Zhu, H. (2017). Rheological properties and anti-aging performance of asphalt binder modified with wood lignin. *Construction and Building Materials*, 151, 801-808.
- [67] Haghshenas, H. F., Haghshenas, D. F., Kim, Y. R., & Morton, M. (2018). *Kinetic analysis of laboratory aging of asphalt binder due to varying thermal-oxidative conditions* (No. 18-02480).
- [68] Feng, Z. G., Bian, H. J., Li, X. J., & Yu, J. Y. (2016). FTIR analysis of UV aging on bitumen and its fractions. *Materials and Structures*, 49, 1381-1389.
- [69] Raviadaran, R., Chandran, D., Shin, L. H., & Manickam, S. (2018). Optimization of palm oil in water nano-emulsion with curcumin using microfluidizer and response surface methodology. *Lwt*, 96, 58-65.
- [70] Khedmati, M., Khodaii, A., & Haghshenas, H. F. (2017). A study on moisture susceptibility of stone matrix warm mix asphalt. *Construction and Building Materials*, 144, 42-49.
- [71] Omranian, S. R., Hamzah, M. O., Yee, T. S., & Mohd Hasan, M. R. (2020). Effects of short-term ageing scenarios on asphalt mixtures' fracture properties using imaging technique and response surface method. *International Journal of Pavement Engineering*, 21(11), 1374-1392.
- [72] Rezaee, M., Khoie, S. M. M., Fatmehsari, D. H., & Liu, H. K. (2011). Application of statistical methodology for the evaluation of mechanically activated phase transformation in nanocrystalline TiO₂. *Journal of alloys and compounds*, 509(36), 8912-8916.
- [73] Hurley, G. C., & Prowell, B. D. (2006). Evaluation of Evotherm for use in warm mix asphalt. *NCAT report*, 2(06).
- [74] Kandhal, P. S., & Chakraborty, S. (1996). Effect of asphalt film thickness on short-and long-term aging of asphalt paving mixtures. *Transportation Research Record*, 1535(1), 83-90.
- [75] Hagos, E. T. (2008). *The effect of aging on binder properties of porous asphalt concrete*.
- [76] Sui, C., Farrar, M. J., Harnsberger, P. M., Tuminello, W. H., & Turner, T. F. (2011). New low-temperature performance-grading method: Using 4-mm parallel plates on a dynamic shear rheometer. *Transportation Research Record*, 2207(1), 43-48.

- [77] Sui, C., Farrar, M. J., Tuminello, W. H., & Turner, T. F. (2010). New technique for measuring low-temperature properties of asphalt binders with small amounts of material. *Transportation research record*, 2179(1), 23-28.
- [78] Qin, Y., Zhang, X., Tan, K., & Wang, J. (2022). A review on the influencing factors of pavement surface temperature. *Environmental Science and Pollution Research*, 29(45), 67659-67674.